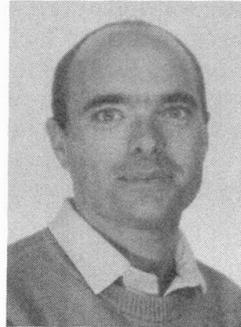# Theme C

Model Updating

Leere Seite

Blank page

Page vide

Traffic Action Effect Reduction Factors for Bridge Evaluation

Simon F. BAILEY
Research Engineer
ICOM-Steel Structures, EPFL
Lausanne, Switzerland

Simon Bailey, born in 1963, graduated from Southampton University, UK, in 1984 and joined a firm of consulting engineers where he worked on the design, construction, and maintenance of structures. Since 1990 he has been conducting research into bridge evaluation at ICOM where he obtained his doctoral degree in 1996.

Summary

This paper presents a simple method for modifying the Swiss design traffic load model in order to take account of the difference between "design traffic" and the actual traffic which uses a given road bridge. This method can be used for the evaluation of structural safety and involves the use of a reduction factor derived as a function of six traffic characteristics which are calculated from site measurements. The paper also describes the development of the method and presents an example of its application.

1. Introduction

1.1 Background

Road-traffic design load models are inherently conservative because of the high uncertainty about traffic loads at the design stage. Furthermore, models must be valid for structures of all types and spans. The increased cost of construction due to the use of a conservative design load model is small and necessary to allow for uncertainty and to simplify the design process. However, once a structure is in service, the cost of an over-conservative evaluation could be much greater, and thus justifies the consideration of actual traffic and the effects it produces. There are thus two important differences between bridge design and evaluation, that is before and after a structure is in service :

design : high uncertainty

evaluation : high cost of increasing safety

Considering actual traffic during bridge evaluation can reveal the extent to which a bridge may have been over-designed through using a conservative traffic load model. In this way, maintenance needs within a bridge stock can be ranked more accurately and unnecessary strengthening or traffic restriction might be avoided.

The main aim of research recently completed at ICOM was therefore to develop a simple method for the consideration of site specific traffic loads as a function of parameters describing the bridge and traffic, referred to as site characteristics. This method is based on a site specific probabilistic model of traffic action effects derived from the results of computer simulations of

traffic effects. The simulation program was used to generate random traffic actions for defined traffic conditions and the frequency distribution of maximum static effects was subsequently determined. The results of more than 1600 simulations were then used to derive empirical relationships between site characteristics and the parameters of a type III extreme value distribution of maximum effects. This paper explains how this probabilistic model has been used in order to develop a simple method for considering site specific traffic actions. This simple method is based on the application of reduction factors to action effects calculated using the Swiss design traffic load model. The paper is a summary of part of a doctoral thesis [1] and describes the innovative approach which was adopted for calibrating reduction factors using probabilistic methods considering various failure modes of bridge structures.

1.2   Considering actual traffic for bridge evaluation

The research described in detail in [1] has led to the development of two methods for considering actual traffic for bridge evaluation ;

- a site specific model of the frequency distribution of extreme traffic action effects,

- a simple method for modifying the effects of the design load model as a function of parameters describing the bridge and traffic, referred to as site characteristics.

The site specific model of the frequency distribution of extreme traffic action effects could be used in bridge reliability analyses for the evaluation of structural safety. However, practising engineers are rarely familiar with probabilistic methods and a simple method for considering actual traffic was therefore developed. This simple method is based on the application of a reduction factor to effects calculated using the Swiss design traffic load model. A reduction factor, α_Q, can be determined as a function of six traffic characteristics, and then applied to the traffic action effects in the following general expression :

$$S_d = S(\gamma_G \cdot G_m) + \frac{S(\gamma_Q \cdot Q_r)}{\alpha_Q} \leq \frac{R}{\gamma_R}$$
(1)

The use of the simple method in practice requires some knowledge of the traffic using the bridge which is being evaluated. Traffic data can be collected using weigh-in-motion techniques [2]. Data has to be analysed in order to calculate the mean, standard deviation and maximum value of heavy-vehicle linear-weights allowing for dispersion due to errors in the measurement systems.

1.3   Development

The site specific model of the frequency distribution of extreme traffic action effects was developed as the first stage of the research. This model was subsequently used in a second stage which consisted of calibrating reduction factors for the simple method. The site specific model of the frequency distribution of extreme traffic action effects has been based on the results of a traffic simulation program. The simulation program generates random traffic loads for defined traffic conditions and determines the frequency distribution of maximum static effects, as described in [1].

In the second stage of research, the site specific model of the frequency distribution of extreme traffic action effects was used in reliability analyses to calibrate reduction factors for the simple method for considering site specific traffic actions. Reduction factors were calibrated for different types of hypothetical traffic, bridge and action effect, as described in Section 2.2. A parametric study then enabled the identification of relationships between reduction factor and site characteristics. The simple method incorporates the relationships for the six most important traffic characteristics.

2. Traffic action effect reduction factors

2.1 Bridge evaluation with partial load factors and reduction factors

The evaluation of existing bridges will not usually be based on reliability analyses since practising engineers are not familiar with probabilistic methods. The site specific model of the frequency distribution of traffic action effects presented in [1] will only rarely be used during bridge evaluation. However, practising engineers are familiar with the partial factor approach to bridge design, and thus this is the most suitable format for bridge evaluation. There is therefore a need to introduce the concept of a site specific traffic load model into the partial factor approach to the assessment of structural safety. It was therefore decided to base the consideration of actual traffic on the Swiss design traffic load model and to propose reduction factors to be applied to it as a function of site characteristics. This reduction factor thus represents the difference between the design traffic which the design load model represents and the actual traffic which uses a given road bridge. Verification criteria would thus have the form of Equation (1). This section presents the calibration of these reduction factors using probabilistic methods and the simple method which was developed for deriving reduction factors as a function of site characteristics.

2.2 Calibration of reduction factors

Reduction factors were calibrated by comparing the frequency distribution of maximum effects due to a hypothetical traffic to that of the design traffic. The Swiss design traffic load model was developed using probabilistic methods and the type of traffic that it represents is thus known [3]. For a given action effect (support moment, midspan moment or support shear) and a defined bridge (span, construction type), the frequency distributions of maximum traffic action effects were derived using the site specific model developed in [1] for both the design traffic and a hypothetical actual traffic. Calibration then consisted of finding a reduction factor, α_Q, such that the frequency distribution of design traffic effects divided by α_Q was "equivalent" to the frequency distribution of hypothetical actual traffic effects, as shown in Figure 1. This figure illustrates the probabilistic approach, considering traffic actions and live load carrying capacity, which was used to determine the "equivalence" of frequency distributions. The figure shows that rather than simply considering a statistical characteristic of the traffic action effect frequency distributions, "equivalence" is defined as equal reliability. Reliability was estimated using the FOSM method by considering the frequency distribution of live load carrying capacity of the hypothetical bridge in a limit state function appropriate to the type of bridge and action effect being considered. This approach is explained in more detail in [1].
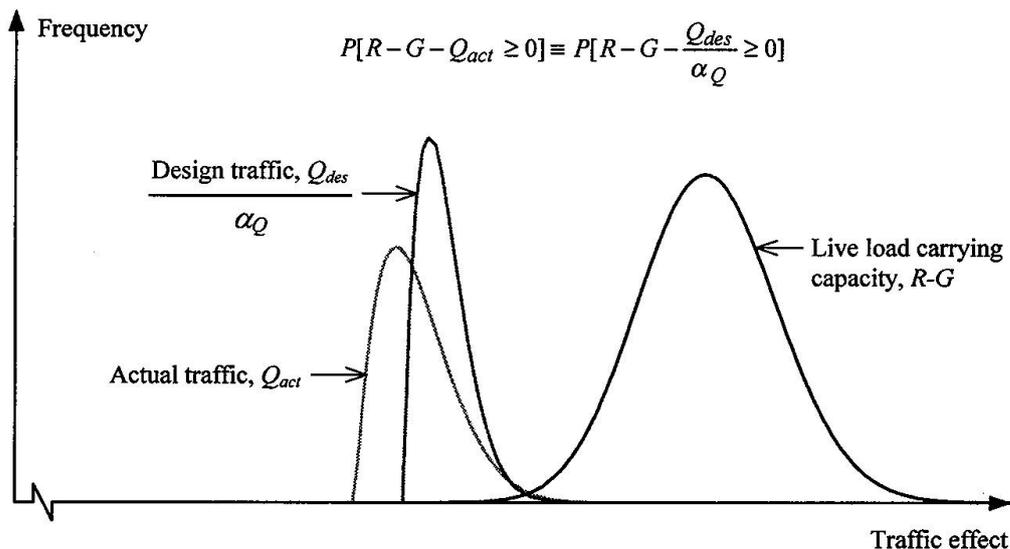

$$P[R - G - Q_{act} \geq 0] \equiv P[R - G - \frac{Q_{des}}{\alpha_Q} \geq 0]$$

Fig. 1 Calibration of traffic action effect reduction factors

The calibration procedure was repeated for different types of traffic, bridge and action effect in order to enable a parametric study of the relationships between reduction factor and site characteristics. Figure 2 presents an example of the results of the calibrations, and shows the variation of reduction factor, α_Q, as a function of the mean value of heavy-vehicle linear-weight, μ_q, with all other traffic characteristics equal to those of the design traffic. The results for two lanes of traffic on many different types of composite bridge and action effect are shown. One bound is defined by the relationship for the support moment in a continuous box-section bridge with spans of 50, 70 and 50 m. The second bound is defined by the relationship for the midspan moment in a continuous slab-on-beam bridge with spans of 22, 30 and 22 m. The figure shows an inverse relationship, with the reduction factor increasing as the mean value of heavy-vehicle linear-weight decreases. The reduction factor is equal to 1.0 when μ_q is equal to the 'design' value of 14.5 kN/m.
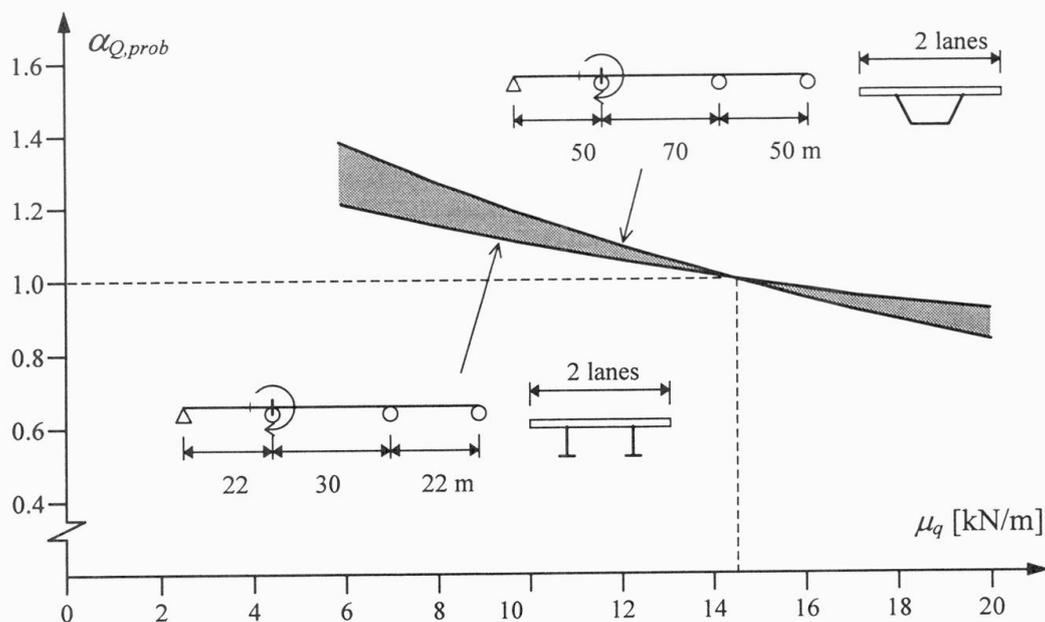

Fig. 2 *Variation of reduction factor as a function of the mean value of heavy-vehicle linear-weight*

The combined and individual influences of 13 different site characteristics were considered in the parametric study. Quantitative relationships between individual parameters and traffic action effect reduction factor were established and the most important characteristics were identified. The next section presents the simple method for determining reduction factors which was developed using these relationships.

2.3   Simple method for determining traffic action effect reduction factors

The individual influences of site characteristics are not independent and it is therefore not possible to consider the combined influence of all traffic characteristics by simply multiplying the appropriate individual reduction factors. However, on the basis of the individual influences it was determined that only the following traffic characteristics need to be considered in a simple method :

- maximum value of heavy-vehicle linear-weight, q_{max}
- mean value of heavy-vehicle linear-weight, μ_q
- standard deviation of heavy-vehicle linear-weight, σ_q
- proportion of heavy-vehicles in the traffic, *HV*
- volume of traffic, *N*
- percentage of free-moving traffic, *F*

A relationship involving these six traffic characteristics was developed by a combination of trial and error and least squares fitting in order to obtain the best agreement with the calibrated reduction factors. It was found that the simple multiplication of individual reduction factors produced errors which increased as traffic characteristics diverged further from the design traffic values. Setting limits on the validity of the relationship and dividing the product of individual factors by the average factor was found to be the most efficient way of ensuring that, in the majority of cases, inaccuracy lead to the under-estimation of a reduction factor.

The following six expressions were derived to model the influence of the most important traffic characteristics (range of validity shown in brackets) :

$$c_1 = \frac{q_{max}}{73} \cdot 0.2 + 0.8 \qquad \left(40 \leq q_{max} \leq 80\right) \qquad (2)$$

$$c_2 = \frac{1}{\frac{\mu_q}{14.5} \cdot 0.65 + 0.35} \qquad \left(6 \leq \mu_q \leq 20\right) \qquad (3)$$

$$c_3 = \frac{1}{\frac{\sigma_q}{6.0} \cdot 0.6 + 0.4} \qquad \left(2 \leq \sigma_q \leq 8\right) \qquad (4)$$

$$c_4 = \frac{1}{\frac{HV}{0.25} \cdot 0.7 + 0.3} \qquad \left(0.1 \leq HV \leq 0.4\right) \qquad (5)$$

$$c_5 = \frac{1}{\log(N) \cdot 0.08 + 0.33} \qquad \left(10^5 \leq N \leq 10^9\right) \qquad (6)$$

$$c_6 = \frac{F}{94} \cdot 0.2 + 0.8 \qquad \left(40 \leq F \leq 100\right) \qquad (7)$$

The coefficients calculated using Equations (2) to (7) are then combined using the following expression in order to determine the appropriate traffic action effect reduction factor :

$$\alpha_Q = \frac{c_1 \cdot c_2 \cdot c_3 \cdot c_4 \cdot c_5 \cdot c_6}{\left(c_1 + c_2 + c_3 + c_4 + c_5 + c_6\right)/6} \qquad (8)$$

Using this simplified method, 95% of the reduction factors, α_Q, are conservative and the remaining 5% do not over-estimate $\alpha_{Q,prob}$ by more than 5%, as illustrated in Figure 3.
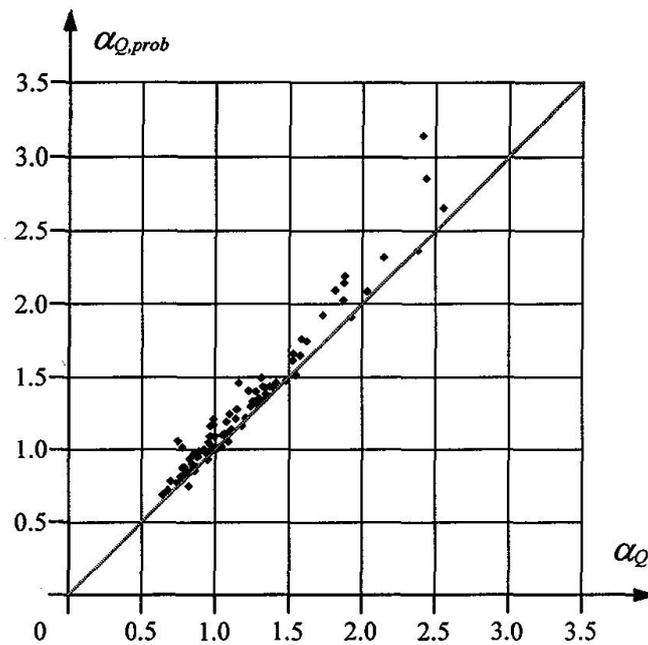
Fig. 3 Comparison of traffic action effect reduction factors derived using the probabilistic approach, $\alpha_{Q,prob}$, and the simple method, α_Q.

3.   Example application of traffic action effect reduction factor

This section presents an example of the derivation of a reduction factor for application to the traffic action effects calculated with the Swiss design load model. The traffic action reduction factor is derived by combining of factors calculated for each of the six traffic characteristics presented in Section 2.3. The first step in using vehicle survey data is thus to determine these traffic characteristics. The maximum value of heavy-vehicle linear-weight should be obtained by fitting a beta distribution to measured data using standard statistical techniques (method of moments, for example). The mean and standard deviation of heavy-vehicle linear-weight should be calculated from data by taking into consideration any bias or dispersion associated with the measurement system. Traffic flow, volume and the proportion of heavy-vehicles are determined from measured vehicle speeds, vehicle counts and classification. The determination of traffic characteristics is illustrated for vehicle survey data collected at the Porte-du-Scex in Switzerland [1]. A histogram of measured heavy-vehicle linear-weights is shown in Figure 4.
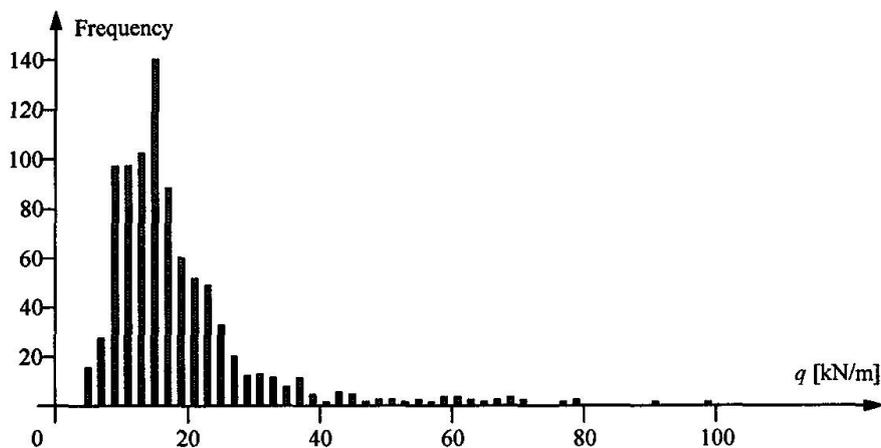

Fig. 4 Histogram of measured heavy-vehicle linear-weight, q

During calibration of the WIMstrip at the Porte-du-Scex site, the system was set up such that there was no bias between measured and actual weights. However, due to the vibration of vehicles as they pass over the WIMstrip as well as other sources of dispersion (only one wheel on each axle is weighed) a measurement error (real linear-weight / measured linear-weight) was noted with a coefficient of variation equal to 0.16. This variation is taken into account when calculating the mean and standard deviation of heavy-vehicle linear-weight, q :

$$\mu_q = \frac{\sum q_{measured}}{n} \tag{9}$$

$$\sigma_q = \sqrt{\frac{\sum q^2_{measured}}{(1+0.16^2)\cdot n} - \mu_q^2} \tag{10}$$

Equations (9) and (10) are only valid because there was no bias to the measurement error. The maximum value of heavy-vehicle linear-weight can be fixed by fitting a beta distribution with a lower bound of 4 kN/m to the measured data considering its first three moments adjusted to allow for a measurement error with the known coefficient of variation.

The values which were determined in this case are given in Table 15. Although traffic at this site was legally restricted to vehicles of less than 16 tonnes, the mean and standard deviation of heavy-vehicle linear-weight are not much lower than that measured on a Swiss highway at Göschenen [4]. However, the proportion of heavy vehicles in the traffic, HV, is very low due to the weight restriction which is imposed.

Traffic characteristic	Notation	Value	Comment
Maximum value of heavy-vehicle linear-weight	q_{max}	70 kN/m	
Mean value of heavy-vehicle linear-weight	μ_q	14 kN/m	
Standard deviation of heavy-vehicle linear-weight	σ_q	6 kN/m	
Traffic flow conditions	A	1 %	at-rest
	C	2 %	40 km/h
	F	97 %	500 veh/h
Traffic volume	N	20 million	10 years
Proportion of heavy-vehicles	HV	0.05	rounded up to 0.1

Table 1 *Traffic characteristics for calculation examples*

Six coefficients are calculated with Equations (2) to (7) using the traffic characteristics given in Table 1. The proportion of heavy vehicles, HV, is rounded up to 0.1, since the simplified method is not valid if HV is less than 0.1. Rounding up the value of HV will lead to a conservative value for the reduction factor.

$$c_1 = \frac{q_{max}}{73}\cdot 0.2 + 0.8 = \frac{70}{73}\cdot 0.2 + 0.8 = 0.99 \tag{2}$$

$$c_2 = \frac{1}{\dfrac{\mu_q}{14.5}\cdot 0.65 + 0.35} = \frac{1}{\dfrac{14}{14.5}\cdot 0.65 + 0.35} = 1.02 \tag{3}$$

$$c_3 = \frac{1}{\frac{\sigma_q}{6.0} \cdot 0.6 + 0.4} = \frac{1}{\frac{6.0}{6.0} \cdot 0.6 + 0.4} = 1.0 \tag{4}$$

$$c_4 = \frac{1}{\frac{HV}{0.25} \cdot 0.7 + 0.3} = \frac{1}{\frac{0.10}{0.25} \cdot 0.7 + 0.3} = 1.72 \tag{5}$$

$$c_5 = \frac{1}{\log(N) \cdot 0.08 + 0.33} = \frac{1}{\log(20 \cdot 10^6) \cdot 0.08 + 0.33} = 1.09 \tag{6}$$

$$c_6 = \frac{F}{94} \cdot 0.2 + 0.8 = \frac{97}{94} \cdot 0.2 + 0.8 = 1.01 \tag{7}$$

and then ;

$$\alpha_Q = \frac{c_1 \cdot c_2 \cdot c_3 \cdot c_4 \cdot c_5 \cdot c_6}{(c_1 + c_2 + c_3 + c_4 + c_5 + c_6)/6} \tag{8}$$

$$= \frac{0.99 \cdot 1.02 \cdot 1.0 \cdot 1.72 \cdot 1.09 \cdot 1.01}{(0.99 + 1.02 + 1.0 + 1.72 + 1.09 + 1.01)/6} = \frac{1.91}{1.14} = 1.68$$

This example illustrates that the determination of traffic action effect reduction factors is simple and that in certain cases a significant reduction is determined. The frequency distribution of heavy-vehicle linear-weight at the Porte-du-Scex is very similar to that of the Swiss 'design' traffic. For this reason the first three coefficients are close to 1.0. Similarly, the proportion of free-moving traffic is close to the 'design' value, and therefore has little influence on α_Q. In this case, the reduction factor of 1.68 is largely due to the low proportion of heavy-vehicles in the traffic.

4.   Conclusions

Site measurements can be made during bridge evaluation in order to reduce the uncertainty about loads and resistance. In particular, the consideration of actual traffic and the effects it produces in a road bridge enables a more accurate assessment and a better ranking of maintenance needs.

A simple method for modifying the effects of the Swiss design load model as a function of traffic characteristics has been developed. This method involves the application of reduction factors to traffic action effects calculated with the design load model. It is applicable to verifications of structural safety based on longitudinal shear and moment effects determined by the simultaneous presence of at least two heavy-vehicles. Traffic action effect reduction factors are determined as a function of site characteristics using the equations presented in Section 2.3. The determination of reduction factors using these equations requires knowledge of the following six traffic characteristics:

* maximum value of heavy-vehicle linear-weight

* mean value of heavy-vehicle linear-weight

* standard deviation of heavy-vehicle linear-weight

* traffic volume

* proportion of heavy vehicles in the traffic

* percentage of free-moving traffic.

The simple method for considering actual traffic can be easily applied in practice with traffic data gathered using Weigh-in-motion techniques. The use of a site specific traffic load model rather

than a design load model means that unnecessary repairs or traffic restriction can be avoided, leading to a better allocation of resources and an optimal use of the maintenance budget.

Acknowledgements

Notation

α_Q	traffic action effect reduction factor
F	percentage of free-moving traffic
γ	partial factor (indices G, Q and R for permanent loads, traffic loads and resistance respectively)
G_m	average value of permanent actions
HV	proportion of heavy-vehicles in the traffic
μ_q	mean value of heavy-vehicle linear-weight
N	volume of traffic
q_{max}	maximum value of heavy-vehicle linear-weight
Q_r	representative value of traffic actions
R	resistance
$S(..)$	effect of actions
S_d	design load effect
σ_q	standard deviation of heavy-vehicle linear-weight

References

1   BAILEY, S. F. Basic principles and load models for the structural safety evaluation of existing bridges, Thesis No 1467, École Polytechnique Fédéral de Lausanne, 1996

2   Pre-proceedings of the First European Conference on Weigh-In-Motion of Road Vehicles, Zurich, 1995

3   BEZ, R. Modélisation des charges dues au trafic routier, Thèse No. 793, École Polytechnique Fédérale de Lausanne, 1989

4   PEEKER, E., BAILEY, S. F., BEZ, R. AND BASSETTI, A. Dépouillement et analyse des mesures du trafic routier, Rapport de mandat No. 657-1, ICOM, École Polytechnique Fédérale de Lausanne, 1995

Leere Seite

Blank page

Page vide

A simplified Model for the Reliability-Based Evaluation of Fatigue in Existing Bridges

Joan R. CASAS
Associate Professor
School of Civil Eng.
Barcelona, Spain
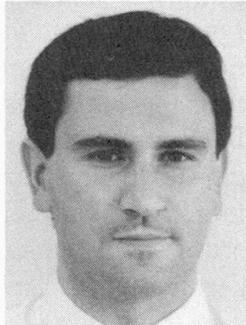
Joan R. Casas, born in 1960, received his civil eng. degree from the Tech. Univ. of Catalunya (UPC) in 1984, where he completed his doctorate in 1988. His research includes dynamics and field testing of bridges as well as bridge reliability

César CRESPO
Research Assistant
School of Civil Eng.
Barcelona, Spain

César Crespo-Minguillón, born 1969, got his civil eng. degree from the Tech. Univ. of Catalunya (UPC) in 1992. He completed his doctorate at UPC in 1996. His research field is the reliability of partially prestressed bridges.

Summary

The paper presents a simplified probabilistic live load model based on the results of a more general model for the simulation of traffic flow over highway bridges developed by the authors [1]. The model, suitable for the fatigue evaluation due to traffic actions, takes advantage of the fact that the rainflow method only uses information about local extremes. The comparison of the results of this simplified model with the general model for a wide range of bridge types, demonstrates its sufficient accuracy and feasibility for practical reliability evaluation purposes.

1. Introduction

The process of evaluation of a bridge clearly involves two separate parts: the updating of the actual resistance and of the loading characteristics, as they can be different from those assumed in the design. Concerning the load part and because the traffic is the most important external action leading to fatigue in short and medium span bridges, to perform a fatigue evaluation it is of principal importance to know the actual stress increments caused by this action during the service life. This can be only achieved via a global model for the continuous traffic flow simulation over the bridge and using the site-specific characteristic of the traffic in or close to the bridge location. However, such a model, formulated in probabilistic terms, is quite complicated and very costly in computational terms. As a consequence, its use in the practical reliability based evaluation of a bridge can be excesively cumbersome and, therefore, rejected. Because of that, a simplified probabilistic live load model, based on the results of a global model for the simulation of the traffic fatigue effects in simply supported and continuous bridges was developed. In this way, a practical and easy application of the fatigue evaluation methods based on Structural Reliability can be performed .

2. Theoretical basis and description of the model

Traffic action on bridges represents a continuous effect in time. In [1] a complete model for continuous traffic flow simulation was developed. To take into account the most important

uncertainties present and to obtain an almost continuous in time history of the traffic effects in the bridge, the general model requires an important computational effort that makes it not suitable for practical evaluation purposes. However, for the traditional fatigue analysis based on the number and magnitude of the increments of the studied effects, the temporal scale provides no information. In fact, the most common method used for cycle counting, the rainflow method, only needs information about the local extremes (local maximums and minimums, Figure 1).
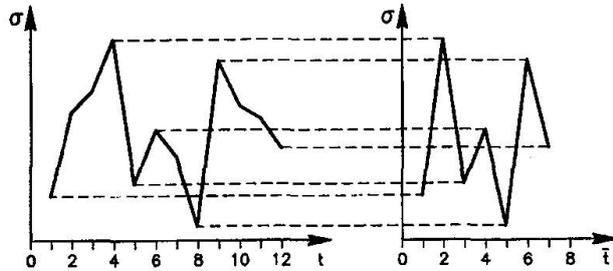
Since the sequence of these diagrams of effects that are the base for the later fatigue reliability analysis, is always the same: a local maximum followed by a local minimum, it was thought that it might be worth to study the possibility of deriving an algorithm for the simulation of these special histories of effects. The analysis of the stochastic process"maximum local extremes" [1] showed an immediate drop in the autocorrelation function and that there will not be any dominant frequency in the spectral density function of the process [1]. Thus, it can be concluded that the analysed process, may be treated as a simply random variable. If the Cumulative Distribution Function (CDF) of the extreme maximum effect value were known, it would be very simple to generate a simulated history of this variable.

Fig. 1 *Two equivalent diagrams of effects*

In figure 2, the pairs (maximum effect, difference between maximum and next minimum effect), for a simply supported and for a continuous bridges are presented. In both cases, a clear linear relationship between the two variables can be seen. It follows that from the history of maximums effects, it should not be very complicated to determine the minimum associated to each maximum. The same effect was observed in many other simply supported and continuous bridges analysed [1].
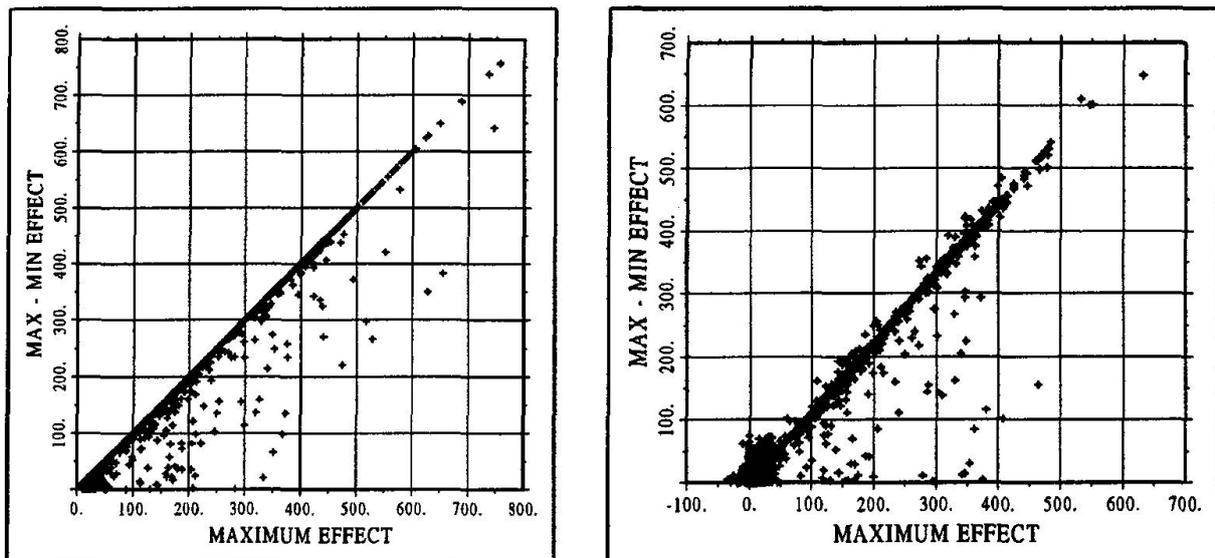
Fig. 2 *Plot of increments of effect vs maximum effect for a simply supported (left) and a continuous (right) bridges*

Next step in the construction of the model consists of the elimination of the transverse structural behavior of each particular deck from the data that will be the base for the model. After several studies, it was decided to use a vehicle type for taking out the dimensions of all recorded histories of traffic. The vehicle was also used for the calculation of the slope of the straight line reflecting the linear relationship between maximum local effects and corresponding increments of effects (Figure 2). The comparison between the real measured slopes and that calculated with this procedure for five continuous bridges with maximum spans from 22 to 150 m, is presented in table 1.

Bridge	Real slope	Calc. slope
S1622	1.149	1.153
S2033	1.201	1.195
B4256	1.167	1.151
C4080	1.107	1.103
C75150	1.103	1.096

Table 1 Relation between the increment of effects and maximum effects

Looking at figure 2, it comes out that the relation between maximums effects and increments of effects, is not exactly linear and deterministic. The deviations of the increments variable around the value given by the deterministic linear relation have been studied. The conclusion is that these deviations can be modelled as a random normally distributed variable with mean equal to 1.0 and COV of 5% in all cases.

The fatigue studies performed showed that only the ranges in the highest levels of stress do really condition the results of the final external fatigue solicitation. Therefore, it was decided to concentrate all efforts in a good definition of the CDF of the non-dimensional local maximum effect, but eliminating the effects caused by light vehicles. The reference value for the effect of a light vehicle was set as a proportion of the 11% of the effect caused by the vehicle type. Next step consisted of studying the extreme maximums higher than the light vehicle limit effect and accomplishing the condition of having minimums after them that lead to effect ranges on the fictitious straight line, (max. effect- range of effect), commented above. The result of this analysis was a CDF of the non-dimensional maximum effects greater than the limit, and a proportion of the number of maximums accomplishing the condition over the total number of lorries expected to cross over the structure. This was done for all bridges, analysing the results from the original model for the simulation of traffic flows. Eleven weeks of simulated traffic results were used.The results for a particular traffic condition are presented in table 2 and figure 3

The average number of lorries per simulated week was calculated to be 41585. So the number of maximum peaks could be thought as a proportion of this average number of expected trucks. It is interesting to realise that the number of maximum extreme situations in the bridges decreases with the length of the deck. This effect is because the probabilities of having situations of several vehicles over the same span of the bridge are higher in long span than in short span bridges.

After seeing the shape of the cumulative distributions functions of maximum non-dimensional peaks (figure 3), it was decided to approximate them in several intervals. The definition of the points of the curves limiting the intervals would be done based on the length of the main spans of the bridges. Given that the curves for the simply supported bridges of lengths 27 and 40 m did not alternate well with the curves of the continuous bridges of close span lengths, it was decided to study both structural types by separate. The study is also divided in two cases of traffic: heavy (Average Daily Traffic of 20,000 vehicles in two lanes with 30 % of trucks) or light (ADT= 10,000 and 15 % of trucks) traffic conditions. In the following, the different parts and steps for the definition of the simplified model are presented.

Bridge	Num of spans	Max. span (m.)	Weekly average number of max. peaks
S1622	3	22	40362
S2033	4	33	39812
B4256	3	56	34303
C4080	3	80	33173
C75150	3	150	27733
S27	1	27	39375
B40	1	40	37939

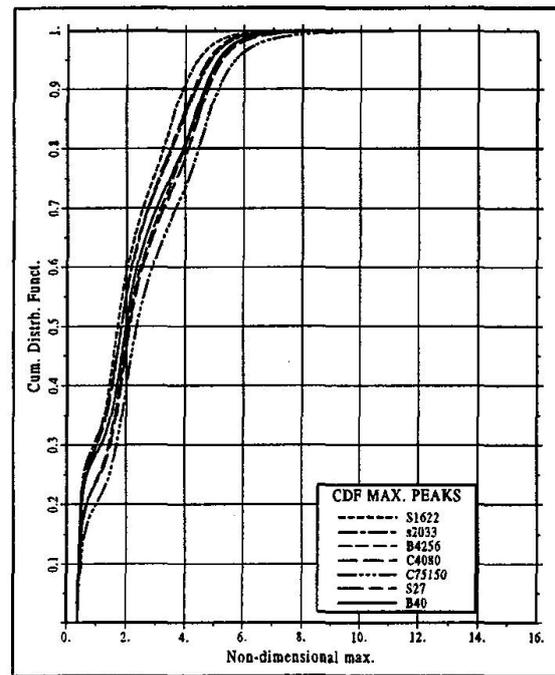**Table 2** *Non-dimensional maximum peaks higher than light vehicle effect limit*

Fig 3 Cumulative distribution functions of the non-dimensional effect at midspan .

2.1 Definition of number of simulations

The first step consists of the definition of the number of maximum effects to be simulated. It is given as a proportion of the average number of expected lorries in a week. In table 3, the results of the simulation of traffic flow are presented for the two traffic conditions.

Bridge	Type	Span length (m.)	Heavy traffic ($N_{trucks} = 41585$)		Light traffic ($N_{trucks} = 10384$)	
			Weekly N. of peaks	Proportion over N. of trucks	Weekly N. of peaks	Proportion over N. of trucks
S1622	C	22	40362	0.9706	14461	1.3927
S2033	C	33	39812	0.9574	14971	1.4418
B4256	C	56	34303	0.8249	12859	1.2384
C4080	C	80	33173	0.7977	12619	1.2153
C75150	C	150	27733	0.6669	11655	1.1224
B19	SS	19.6	39934	0.9603	14580	1.4041
S27	SS	27	39375	0.9469	13987	1.3470
B40	SS	40	37939	0.9123	13385	1.2890

C= continuous, SS = simply supported

Table 3 *Relation between the number of peaks and the number of expected trucks*

With the results in table 3, the total number of major maximum extremes to simulate (N_{peaks}) as a function of the total number of expected trucks in a week (N_{trucks}) and the maximum span length of the bridge, can be derived using the expression:

$$\frac{N_{peaks}}{N_{trucks}} = a + b\ L + c\ L^2 \tag{1}$$

The coefficients in equation (1) are shown in table 4 depending on the traffic conditions and bridge type.

Bridge type	Traffic	a	b	c
SS	Heavy	0.9698	3.78e-4	-4.54e-5
	Ligth	1.6159	-1.37e-2	1.37e-4
C	Heavy	1.0772	-4.77e-3	1.36e-5
	Ligth	1.5522	-6.06e-3	2.13e-5

Table 4 *Values of parameters in equation 1. (SS= simply supported, C=continuous)*

2.2   Obtention of the CDF

Once the number of peaks to simulate in each case was known, the next step consisted on the definition of the Cumulative Distribution Function of the variable "non-dimensional local maximum" to be used in the simulation. It was decided to split the function in different intervals. According to figure 3, where the real CDF for the different cases are presented, and to better approximate each case, the limits of the intervals are different depending on the bridge type and traffic conditions. From the different cases studied, it was derived that less of the 10% of the increments of effects had an effective and practical influence on the final fatigue damage. Therefore, it was decided to give the low parts of the CDF through some straight lines, and to concentrate all efforts in the correct definition of its highest part, causing the relevant values. In this way, in tables 5 to 8, the analytical expressions that best fit the real non-dimensional maximums corresponding to the limits of the different intervals in the CDF are given. As an example, in figure 4 the shape of the analytical expression for the case of continuous bridges and heavy traffic conditions is presented and compared to the values of the real CDF.
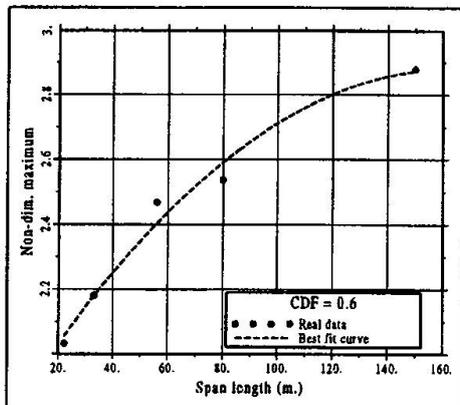
As it was previously explained, the highest efforts were put in the study of the upper tail of the CDF because these are the effects that mostly contribute to the final fatigue damage. The main problem was to choose an analytical expression that were easy to deal with and also, accurate enough to represent the highest effects of traffic. Related to this accuracy, it was intended that the simulated CDF led not only to good estimations of the fatigue life of all studied structures, but also that predicted a histogram of high effects similar to that given by the true simulation of traffic flow.

Fig. 4 Shape of expression CDF = 0.6

CDF	Analytical expression
$0.2^{(1)}$	$0.3799+3.9593 \cdot 10^{-3} \cdot L$
0.4	$01.1928+1.1355 \cdot 10^{-2} \cdot L - 3.7492 \cdot 10^{5} \cdot L^2$
0.6	$1.7802+1.3392 \cdot 10^{-2} \cdot L - 4.0710 \cdot 10^{-5} \cdot L^2$
$0.925^{(2)}$	$3.1652+5.8923 \cdot 10^{-2} \cdot L - 6.2092 \cdot 10^{-4} \cdot L^2 +2.1735 \cdot 10^{-6} \cdot L^3$
0.999997	$13.8168-8.0269 \cdot 10^{-4} \cdot L + 9.9336 \cdot 10^{-5} \cdot L^2$

CDF	Analytical expression
$0.3^{(1)}$	$- 0.369+7.8954 \cdot 10^{-2} \cdot L - 1.0234 \cdot 10^{-3} \cdot L^2$
0.7	$0.2358 + 0.1389 \cdot L - 1.7454 \cdot 10^{-3} \cdot L^2$
$0.925^{(2)}$	$2.4488 + 0.1100 \cdot L - 1.2480 \cdot 10^{-3} \cdot L^2$
0.999997	$12.0463+2.4992 \cdot 10^{-2} \cdot L + 5.3353 \cdot 10^{-4} \cdot L^2$

Table 5 *Analytical expressions of the NDMs as a function of the main span length (L).Heavy traffic* and *continuous bridges.*

Table 6 *Analytical expressions of the Non-Dimensional Maximums (NDMs). Heavy traffic and simply supported bridges*

CDF	Analytical expression
$0.3^{(1)}$	$0.3080 + 6.6277 \cdot 10^{-3} \cdot L - 1.9895 \cdot 10^{-5} \cdot L^2$
0.7	$1.8373 + 1.7929 \cdot 10^{-2} \cdot L - 6.5435 \cdot 10^{-5} \cdot L^2$
$0.95^{(2)}$	$2.3728 + 0.1201 \cdot L - 2.0051 \cdot 10^{-3} \cdot L^2 + 1.4020 \cdot 10^{-5} \cdot L^3 - 3.4392 \cdot 10^{-8} \cdot L^4$
0.999994	$13.4615 - 7.8838 \cdot 10^{-3} \cdot L + 7.0042 \cdot 10^{-5} \cdot L^2$

CDF	Analytical expression
$0.4^{(1)}$	$- 1.1182 + 0.1292 \cdot L - 1.6605 \cdot 10^{-3} \cdot L^2$
0.7	$0.7150 + 8.9375 \cdot 10^{-2} \cdot L - 1.0441 \cdot 10^{-3} \cdot L^2$
$0.95^{(2)}$	$3.0665 + 7.7582 \cdot 0^{-2} \cdot L - 8.1213 \cdot 10^{-4} \cdot L^2$
0.999994	$12.194 + 9.2991 \cdot 10^{-3} \cdot L$

Table 7 *Analytical expressions of the NDMs. Light traffic and continuous bridges*

Table 8 *Analytical expressions of the NDMs. Light traffic and simply supported bridges*

Finally it was decided to study the problem from the rigorous statistical tail approximation theory. The proposal given in [2], for the analysis of the excesses of a variable over a certain threshold, was used. From the simulation results of 200 weeks of traffic, eleven of them (weeks 1,20,40,....,200), were chosen. After taking the transverse effects of each corresponding surface of influence out with the procedure explained before, the final true-assumed Cumulative Distribution Function of the variable non-dimensional maximum local extreme was obtained in a format given by several thousand points. Then, the excesses over the threshold u corresponding to a CDF of 0.925 (heavy traffic)or 0.95 (light) were analysed in a plot representing the function $-log(1. - F_S(s))$ versus the excess s $(s = x-u)$, over the threshold u. S is a new variable: excess of the studied effect X over the threshold u, and $F_S(s)$ is the Cumulative Distribution Function of this new variable. Knowing the CDF of X, $F_X(x)$, the values of $F_S(s)$ are immediate:

$$F_S (s = x - u) = \frac{F_X (x) - F_X (u)}{1.0 - F_X (u)} \qquad (2)$$

For each case, the threshold u is decided based on the value of the initial point of the interval (a $^{(2)}$ in tables 5 to 8), in the way that $F_X(u) = a$. The expression for calculating its simulated value for each main span length, and traffic conditions is given in tables 5 to 8. In this way, any generated random number higher than "a" will be assumed as a realization of $F_X(x)$. With the expression given in equation 2, it will be transformed into a realization of $F_S(s)$. Then, if the analytical

expression of $F_S(s)$ is known, the corresponding value of s could be calculated. Finally, adding the value of s to the threshold u, $x = u + s$, the value of X corresponding to the original random number assumed for $F_X(x)$ will be obtained.

The plots of $-\log(1.- F_S(s))$ versus s show that a parabolic curve fitting is indicated. Therefore, the next step is to obtain the parameters a1 and a2 of the parabolic curve $a1 \cdot s + a2 \cdot s^2$, that best fits the functions $-\log(1.- F_S(s))$ (s = excess over the threshold), in each case. The analytical expressions to obtain the values of a1 and a2 to define the upper part of the simulated CDF, as a function of the main span length (L) for the 4 cases considered, are as follows:

$$al = p + qL + rL^2 \qquad a2 = s + tL + wL^2 \qquad (3)$$

Bridge type	Traffic	p	q	r	s	t	w
SS	Heavy	2.686	-5.313e-2	5.508e-4	-0.172	6.787e-3	-8.526e-5
	Ligth	2.379	6.204e-2	-4732e-4	-0.153	-9.362e-4	5.997e-5
C	Heavy	1.740	-5.229e-3	0	-7.837	8.267e-4	-1.991e-6
	Ligth	2.126	-5.736e-3	3.994e-6	-0.126	6.726e-4	-7.170e-7

Table 9 *Values of parameters in equation 3. (SS= simply supported, C=continuous)*

In figure 5, plots to illustrate the goodness of the analytical expression for a1 and a2 as a function of the main span length, are presented .
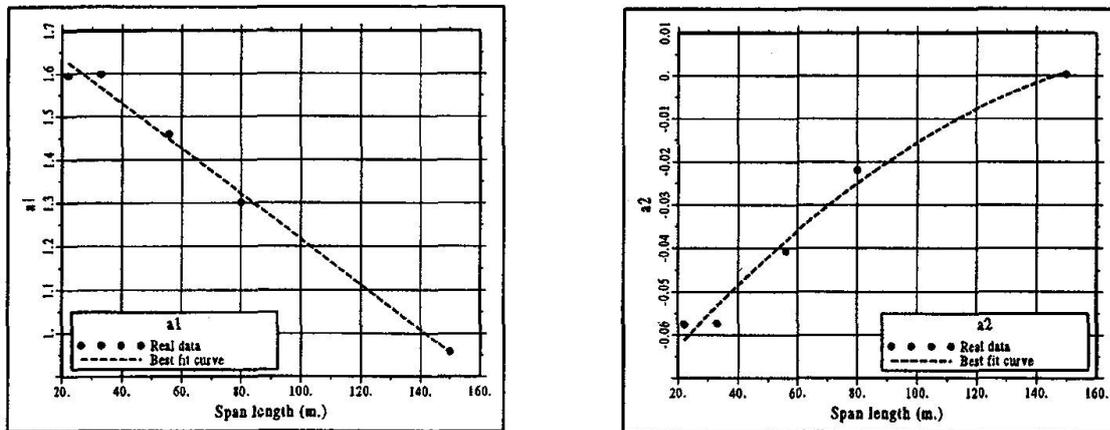

Fig. 5 *Plot of real values of a1 and a2 and best fit curve for the case of continuous bridges and heavy traffic conditions*

Summarizing, the final simulated CDF of the maximum non-dimensional peaks will have five (table 5) or four parts (tables 6, 7 and 8). The first one will have a parabolic shape, the following three (or two) will be straight lines and the last one will have an exponential shape. The simulation algorithm of peaks becomes then, as follows:

1) The first step consists of computing the points and parameters defining the simulated CDF. So the first interval of the simulated CDF will range from CDF = 0.0 to CDF = [1] (see tables 5 to 8).

The value of the variable corresponding to CDF = 0.0, will be $NDM_0 = 0.367$ constant for all span lengths, traffic conditions and bridge type. The Non-Dimensional Maximum (NDM) corresponding to the value at CDF = [1] will be computed with the corresponding expressions in tables 5 to 8. From the plot of the true CDF in figure 3, it can be deduced that a parabola between these two limits of the first interval would fit the real curve better than a straight line. The slope of the CDF function in the origin, has been found to correspond to a value of 0.524, in all cases.

The values of the studied non-dimensional variable corresponding to the rest of milestone points in the simulated CDF, can be easily computed through the expressions given in tables 5 to 8. Then, for the intervals of CDF between the values [1] and [2], straight lines will be assumed.

2) Definition of the parameters governing the shape of the CDF in its upper part. The threshold value, u, of the variable, (the value corresponding to a true CDF of [2] in tables 5 to 8), can be calculated through the expressions given in tables 5 to 8. The parameters of the parabolic curve: $a1 \cdot s + a2 \cdot s^2$ that best fits the function: $-\log(1.-F_s(s))$, where S represents "the excess of X over the threshold", can be calculated with the expression given in equation (3) and table 9. Then, if a randomly generated number greater than $F_X(u) = $ [2] and less than 1, is thought as a realization of $F_X(x)$, the value of its corresponding $F_s(s)$, ($s = x-u$), will be easily calculated through equation (2). Knowing the analytical expression of $F_s(s) = 1.0 - EXP(- a1 \cdot s - a2 \cdot s^2)$, it just rests to solve the second order equation (4) to calculate the value of s (where Fs(s) is already known):

$$a2 \cdot s^2 + a1 \cdot s + \log(1.0 - F_S(s)) = 0. \qquad (4)$$

The final inverse to the generated value of the CDF, will be x = u + s.

2.3   Obtention of extreme traffic effects

At this point, all the information needed for the simulation of a fictitious history of extreme traffic effects at the midspan section has already been given.Summarizing, the steps are:

1)Determination of the total number of major maximum extremes as a function of the total number of expected trucks in a week as described in section 2.1 (use equation (1)).

2) Obtention of the non-dimensional maximum peaks using the proposed CDF, as described in section 2.2, in the simulation process.

3) Multiplication of the non-dimensional peaks by the reference constant effect corresponding to the specific surface of influence for each bridge and the assumed vehicle type. In this way, the dimensional effects are obtained. The reference constant is obtained as the maximum effect that the vehicle type, placed on the axle of the slow lane, would cause when crossing a lone over the surface of influence of the bridge. The vehicle type should be chosen so that the range of nondimensional effects was wide enough as to easily detect the differences between the results from the application of the true simulation model and the simplified model.

4) Building up of the final history of simulated traffic effects following the algorithm explained in figure 2 and using the relationship: slope= (max-min)/max, and considering the randomness reflected in figure 2 through a Normal variable with mean 1 and COV of 5 %. The slope will be calculated from the surface of influence of the bridge and the vehicle type, obtaining the maximum and minimum effects of the vehicle when crossing the bridge.

The simulation algorithm to build the final history of peaks in the case of simply supported bridges is similar to the case of the continuous bridges. In this case, however, because of the shape of the surface of influence of the studied effect, each local maximum leads only to two points in the whole history. These two points are the simulated maximum and the corresponding minimum, this last is set at a value of 0.0.

3.   Verification of the model

To check the reliability of the proposed method, the Reliability Index (β) in front of fatigue, following the methodology presented in [1,3], for different bridges with different typologies, span-lenghts and amounts of prestressing is evaluated using the traffic effects obtained from the complete simulation model of traffic flow and those obtained with the simplified model presented in the paper. The results are summarized in table 10.

Bridge and Section	Heavy traffic		Light traffic	
	β_{comp}	β_{simp}	β_{comp}	β_{simp}
S162201	6.48	6.32	7.16	6.82
S162202	6.78	6.62		
S162203	7.55	7.22		
S203301	6.88	6.91	7.39	7.26
S203302	7.05	7.05		
S203303	7.38	7.27		
B425600	4.63	4.58	5.58	5.39
B425603	6.12	6.14		
B425604	6.40	6.30		
C408000	4.38	4.68	5.36	5.31
C408001	6.37	6.55		
C408002	6.75	6.89		
C7515000	4.25	4.56	5.39	5.52
C7515001	5.22	5.34		
C7515002	6.15	6.22		
S2700	4.30	4.04	5.34	5.21
B4000	4.79	4.71	5.69	5.59

Table 10 Comparison of Reliability Indexes in front of fatigue using a complete traffic flow model and the simplified model

In table 10, the letter S in the bridge definitions stands for slab, B for box-girder and C for box girder bridge built by the balanced cantilever method. The results show the good accuracy got by the application of the simplified model. In the case of continuous bridges and hevay traffic, only in three out of the fifteen cases studied, the differences between the results given by the model for simulation of real traffic flows over bridges and those from the simplified model, are greater than 3%. In the case of simply supported bridges, the slight deviation towards lower safety indexes, is probably due to the fact that no factor has been adopted for correcting the relation between the maximum effect and the corresponding increment. In figure 2, it can be seen that for several cases of high maximums, their following minimum did not take a 0.0 value. So, the final increment of effect was lower than the value adopted by the local maximum. The inclusion of this effect into the simulation would add some difficulties to its application. In the current format, the model is accurate, simple and just slightly conservative.

4.   Conclusions

From the aplication of the proposed model for traffic action, the following conclusions are drawn:

1) The simplified model can be used by researchers and professionals that wish to approximate, in an accurate but not cumbersone and way needing high computational resources and time , the Reliability Index in fron of fatigue of a bridge. The model proposed allows for creating, in a very simple and practical way, fictitiuous histories of traffic effects that can be directly used in the rain-flow algorithm. The relation between the accuracy and the savings in terms of computational costs, provided by this simplified model is very high. Its simpleness makes it very suitable for use in both evaluation and design stages. Furthermore, given the special sensitivity of the studied

problem to the actual values of the external effects, (the stress increments are raised to high power in the corresponding S-N curves for the material), the high accuracy reached with this simplified model indicates that the sequence of high extreme maximums resulting from the application of the model, must be very similar to that from the complete traffic simulation.

2) Because the model is based in the results of a complete traffic flow model over bridges, it includes the two-dimensional effect of bridge decks, the effects of possible multiple presence of vehicles in one and/or several lanes, correlations between vehicles,...In the paper, the parameters of the model for continuous and simply supported bridges are presented. Two extreme cases of traffic are also presented. Other traffic conditions can be easily obtained based on the methodology presented in the paper.

3) Although the model has been derived for the study of fatigue effects in partially postensioned concrete bridges, the methodology outlined makes also extensible the results to bridges with other materials (steel, composite,....) since only the geometry of the bridge is used via its surface of influence.

4) An interesting point of the model is that it automatically introduces the situations of multipresence of vehicles on the bridge. This effect is only included in the most complete and detailed traffic model for fatigue checking given in the Eurocode 1- Part 3., which proposes the use of real records of traffic. The simplified model proposed herein is much simpler and cheaper.

Acknowledgments

References

1.   CRESPO-MINGUILLON, C. A reliability based methodology to define the limit state of decompression in prestressed concrete bridges. Ph.D. Thesis. Technical University of Catalunya. Barcelona, 1996.

2.   MAES, M.A. Tail heaviness in Structural Reliability. Proceedings of Applications of Statistics and Probability ICASP, Paris 1995, 997-1002.

3.   CASAS, J.R.; CRESPO-MINGUILLON, C. Serviceability and fatigue evaluation of existing bridges. Proceedings of the US-Europe Workshop on Bridge Engineeering (Casas, Klaiber and Mari Eds.), Barcelona 1996, 441- 464.

Redundancy of Steel Girder Bridges

Michel GHOSN
Associate Professor
The City College of New York
New York, NY, USA

Michel Ghosn received his Ph.D.
in Civil Engineering from Case
Western Reserve University, in
1984. He joined the City College
of New York in 1985. His
research interests are in the
reliability and load modeling of
bridge structures.

Summary

This paper proposes a framework to include bridge redundancy during the design and evaluation of steel-girder bridges. Redundancy is defined as the capability of a bridge system to continue to carry loads after the failure or the damage of one or more of the bridge's main load carrying members. This paper illustrates how typical design-check equations could be modified by including system factors that account for the level of redundancy inherent in a particular steel bridge configuration. These system factors are calibrated using reliability techniques to ensure that bridge structural systems will provide acceptable levels of structural safety.

1. Introduction

The structural components of a bridge system do not behave independently, but interact with other components to form one structural system. Current bridge specifications generally ignore this system effect and deal with individual components. Since redundancy is related to system behavior, this study proposes a method to close the gap between a component by component design and the system effects. This is achieved by including system factors in the member design equations of bridge superstructures. The system factors are calibrated using reliability techniques based on the nonlinear behavior of steel-girder bridge configurations. This paper reviews the results of the analysis of steel bridges and illustrates how the calibration process is carried out.

2. Nonlinear analysis procedure

The behavior of typical steel I-beam bridges is analyzed using the Nonlinear Bridge Analysis program NONBAN [1]. The program uses a modified grillage analysis method to study the nonlinear behavior of typical bridge configurations. The discretization procedure required is typical for the grillage analysis method as described by Hambly or Zokaie and Imbsen [2,3].

NONBAN requires the linear and nonlinear material properties of each beam element. An element's linear elastic properties include the modulus of elasticity, the moment of inertia, the shear modulus, and the torsional constant. The nonlinear properties are represented by a moment versus plastic rotation curve. The moment versus plastic rotation curve is obtained from the

moment versus curvature relationship by multiplying the curvature by the length of the element. This assumes that the moment and curvature are constant over the length of the beam element.

The moment versus plastic curvature relationship for a steel member is obtained based on the experimental data assembled by Schilling [4]. The experimentally derived curve accounts for steel yielding including: the effect of residual stresses; the spread of yielding along the length of the beam element as the loading progresses; cracking or local crushing of the slab; permanent distortion of the cross sectional shape; and any other factor that causes permanent rotations. The moment curvature relationships for the transverse members representing the contribution of the concrete slab are obtained analytically from the stress-strain curves of the concrete and reinforcing steel bars using section equilibrium. Details about the program NONBAN and the modeling scheme used in this study are provided in Reference [1].

2.   Model verification

The validity of the program NONBAN and the modeling scheme used to study the behavior of steel I-beam bridges is verified by comparing the results of NONBAN to those of two full-scale bridge tests. The first test was performed in Tennessee on a four-span continuous bridge [6]. The bridge consists of four steel W36x170 rolled I-beams at 2.5 m (8.25 ft) spacing supporting a 178 mm (7 in) deck slab. Sections over the piers have cover plates. Loads were placed to simulate one AASHTO HS-20 design truck [5] in each lane of the second span. Figure 1 shows a comparison between the field results published in reference [6] and the results of NONBAN. Excellent agreement is observed for the whole range of loading. This includes the prediction of the yielding load and the ultimate load.

The Nebraska laboratory test was performed on a full scale simple span 21 m (70 ft) bridge [7]. The bridge consists of three steel plate girders at 3m (10 ft) spacing supporting a 190 mm (7.5 in) deck slab. Loads were placed to simulate two side-by-side AASHTO HS trucks. The beams and the slab were built to act as composite sections. Figure 2 shows a comparison between the laboratory results published in reference [7] and the results of NONBAN. Excellent agreement is again observed although the test results show that the ultimate capacity was not reached because punching shear failure occurred in the slab slightly before ultimate load.
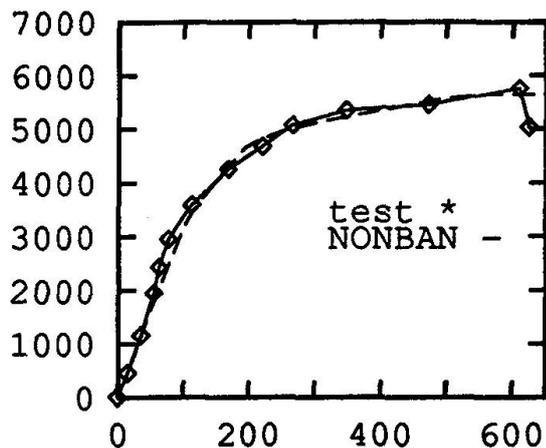
Fig. 1 Comparison of NONBAN
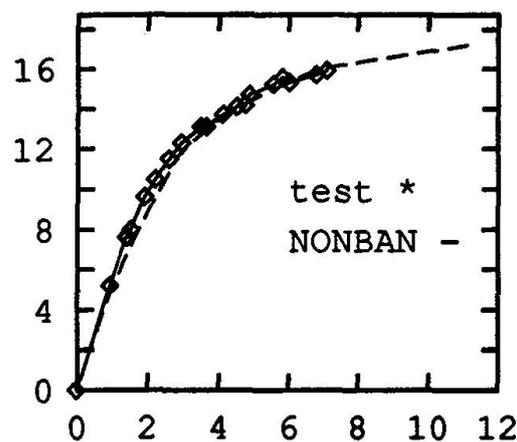   to Tennessee's test [6].

Fig. 2 Comparison of NONBAN
        to Nebraska's test [7].

The comparisons between the results of NONBAN and the two full scale bridge tests as well as other tests reported in reference [1] illustrate the validity of the program and the modelling scheme used in this study. The comparisons confirm that the moment-rotation curves developed in this study based on the experimental data proposed by Schilling [4] provide excellent representations of the actual behavior of steel bridge members.

3. Analysis of typical steel -girder bridge configurations

To study the behavior of typical steel I-beam bridge configurations several steel bridges are designed to cover typical span lengths and cross-sectional configurations. The bridges are designed to satisfy AASHTO's LFD criteria [5]. Simple span bridges as well as continuous two-span bridges with individual span lengths varying between 14 and 46 m (45 and 150 ft) are designed assuming that the deck is supported by 4, 6, 8 or 10 beams with beam spacing varying between 122 and 366 cm (4 and 12 ft). The concrete bridge decks are assumed to vary in depth between 19 and 22 cm (7.5 and 8.5 in) depending on the beam spacing. For each bridge configuration, section dimensions were chosen to satisfy AASHTO' s requirements for beam depths. The beams are assumed to be A-36 steel (f_y= 246 MPa) while the deck's strength, f'_c, is equal to 24 MPa (3.5 ksi).

The nonlinear analysis of these bridge systems is performed using NONBAN. The mesh discretization and models used in this study follow the guidelines given in reference [3]. The beams in the longitudinal direction account for the composite action between the slab and the I-beams. In addition, it is assumed that the bridges have no transverse diaphragms. Hence, the lateral distribution of the load is only affected by the transverse properties of the deck slab.

The dead load is assumed to be uniformly distributed along the length of each longitudinal member. All the longitudinal members are assumed to carry the same dead load. The live load is formed by AASHTO HS-20 vehicles placed longitudinally in the most critical design points. The base case assumes two side-by-side vehicles. No resistance nor load safety factor or dynamic impact factors are applied during the analysis. This is because the purpose of the incremental analysis is to evaluate the capacity of the bridge expressed in terms of how many HS-20 trucks it can carry before it fails. The effect of the dynamic impact is included at a later stage during the reliability analysis.

The AASHTO HS-20 vehicles are incremented until bridge system failure occurs. The load factor at which the system fails is defined as LFu. LFu gives the factor by which the weights of the initial HS-20 vehicles are multiplied to produce system failure. Failure of the bridge is assumed to occur when one main longitudinal member reaches a plastic hinge rotation equal to the maximum allowable plastic rotation. The maximum allowable plastic rotation corresponds to the value at which the concrete crushes or the steel ruptures. It is herein assumed that concrete crushing under transverse bending or in secondary members will only produce local failures. Therefore, no failures in the transverse direction are considered.

In addition to calculating the load factor corresponding to the ultimate capacity of the bridge system (LFu), the load factor corresponding to the level at which the bridge becomes non-functional is recorded. It is assumed that a bridge becomes non-functional when the maximum live load displacement under a main longitudinal member reaches a value corresponding to the span length/100. The load factor corresponding to this displacement level is expressed by the variable LF100. The L/100 value is chosen because it is similar to the values at which many bridge field tests were stopped when the researchers observed potentially dangerous deflections.

Following the calculation of the ultimate capacity of the intact structure, a similar analysis is performed assuming damaged conditions. The damage scenario assumes that the external girder is so heavily damaged that it can no longer carry any load. This simulates a situation where the external girder is knocked out of service due to a collision or fracture. The incremental nonlinear analysis of bridge structures where the external member is assumed to be totally damaged is executed using the same assumptions stated above for the intact structures. The ultimate load capacity for a damaged bridge scenario is designated by the variable LFd.

To provide a measure of a bridge's level of redundancy, the load factor at which the intact bridge system fails (LFu) , the load factor at which the bridge becomes dysfunctional (LF100) as well as the load factor for the damaged bridge scenario (LFd) are compared to the load factor corresponding to the first member failure LF1. LF1 in this case is calculated assuming linear elastic behavior of the bridge members. A linear elastic behavior is assumed in order to be consistent with current member oriented design and analysis procedures. Thus, the LF1 factor represents the estimated bridge member capacity using current traditional member checking methods without consideration of the code-specified safety factors. The calculation of LF1 is performed using the equation:

$$LF_I = \frac{R - D}{DF_I \cdot L\,L_{HS-20}}$$

where R is the member's unfactored moment capacity, D is the member's unfactored dead load, DF_1 is the linear elastic distribution factor for the member assuming linear elastic behavior, and LL_{HS-20} is the total live load moment effect due to the HS-20 vehicles. The product $DF_1 \cdot LL_{HS-20}$ correspond to the highest live load linear moment effect for any longitudinal member.

As an example of the results obtained, Table 1 gives the LFu, LF100, LFd and LF1 factors for the 46 m (150 ft) simple span bridges. Because redundancy is essentially a comparison between the system capacity and that of the individual members, the ratios of LFu/LF1, LF100/LF1 and LFd/LF1 are used as objective deterministic measures of bridge redundancy. These ratios are also shown in Table 1.

		4 beams		6 beams		8 beams		10 beams	
		LF	LF/LF1	LF	LF/LF1	LF	LF/LF1	LF	LF/LF1
4ft	LFu	2.51	1.01	3.55	1.41	3.69	1.46	3.76	1.44
	LF100	2.51	1.01	3.13	1.25	3.25	1.29	3.36	1.29
	LFd	1.45	0.59	2.16	0.86	2.29	0.90	2.29	0.87
	LF1	2.48	-	2.52	-	2.52	-	2.62	-
6 ft	LFu	3.65	1.27	3.90	1.37	4.03	1.36	4.05	1.35
	LF100	3.34	1.16	3.51	1.23	3.68	1.24	3.70	1.23
	LFd	1.61	0.56	1.88	0.66	1.95	0.66	1.95	0.65
	LF1	2.88	-	2.85	-	2.97	-	3.00	-
8 ft	LFu	4.14	1.33	4.42	1.35	4.46	1.35	4.47	1.35
	LF100	3.74	1.20	4.03	1.23	4.09	1.24	4.09	1.24
	LFd	1.47	0.47	1.79	0.55	1.78	0.54	1.73	0.52
	LF1	3.12	-	3.26	-	3.31	-	3.31	-
10 ft	LFu	4.46	1.30	4.78	1.33	4.79	1.33	-	-
	LF100	4.14	1.21	4.45	1.24	4.47	1.24	-	-
	LFd	1.23	0.36	1.39	0.39	1.38	0.38	-	-
	LF1	3.43	-	3.59	-	3.59	-	-	-
12 ft	LFu	4.80	1.27	5.00	1.30	-	-	-	-
	LF100	4.52	1.20	4.74	1.23	-	-	-	-
	LFd	1.06	0.28	1.21	0.31	-	-	-	-
	LF1	3.77	-	3.85	-	-	-	-	-

Table 1 *Results of nonlinear analysis of 46 m bridge*

4.   Sensitivity analysis

In addition to the analysis of the bridges described above, a parametric analysis is performed to study the sensitivity of the results to the assumptions made during the design of the bridge members and during the nonlinear analysis of the structural models. The simply-supported 46 m (150 ft) bridge with 6 beams at 240 cm (8 ft) is used as the base case for the sensitivity analysis.

The results of Table 2 show that the structural model used provides reasonably stable results. Changes in the LFu/LF1, LF100/LF1 and LFd/LF1 ratios are significantly affected by changes in the moment capacity of the longitudinal girders and changes in the dead load. Other factors that are of importance are the moment capacities of the slab and the maximum plastic hinge rotation. Also, it is observed that the effect of changes in the deck slab capacities are insignificant for the intact bridge. Similarly, the presence of diaphragms at each support and the mid-span does not improve the results obtained for the intact bridges. On the other hand, placing a diaphragm at the bridge's mid-span and the strengthening of the deck slab improve the overall system capacity and redundancy of damaged bridges. It is also noted that, although a high increase in the assumed torsional rigidity of the longitudinal beams does not affect the results of the analysis significantly, an increase in the torsional rigidity of the members representing the deck slab produce a noticeable improvement in the LF/LF1 ratios especially for the damaged case. Other results show that increasing the bridge skew does not produce any significant change in the LFu/LF1 ratio of the intact bridge although a reduction in the ratio of damaged bridges is observed. It is also noted that an increase in the longitudinal member capacities will decrease the LF/LF1 ratios.

The results of the simple span bridge are also compared to those of a continuous two-span bridge. The analysis of the continuous bridges shows that the two-span continuous bridges produce higher system redundancy only when the support is provided with sufficient levels of ductility in the negative bending region. This requires the use of compact steel sections over the interior supports.

	LFu	LF100	LFd	LF1	LFu/LF1	LF100/LF1	LFd/LF1
Base case	4.43	4.03	1.79	3.26	1.36	1.24	0.55
Fully composite	4.42	4.03	1.79	3.26	1.35	1.24	0.55
Double long. torsional constant	4.59	4.17	1.91	3.30	1.39	1.26	0.58
Double trans. torsional constant	4.69	4.16	2.11	3.30	1.42	1.26	0.64
Double long. moment of inertia	4.41	4.13	1.76	3.25	1.36	1.27	0.54
Double trans. moment of inertia	4.43	4.07	1.77	3.24	1.36	1.25	0.55
Double long. moment capacity	10.23	8.90	4.10	8.72	1.17	1.02	0.47
Double trans. moment capacity	4.51	4.08	2.02	3.26	1.38	1.25	0.62
Double dead load	1.71	1.51	0.00	1.07	1.60	1.42	0.00
Double maximum hinge rotation	4.86	4.03	2.31	3.26	1.49	1.24	0.71
30 degree skew	4.49	4.08	1.69	3.30	1.36	1.24	0.51
diaphragms at ends	4.42	4.04	1.82	3.26	1.36	1.24	0.56
diaphragms at ends & midspan	4.50	4.12	2.05	3.30	1.36	1.25	0.62

Table 2 Results of Sensitivity Analysis.

5.   Reliability analysis and calibration of redundancy factors

5.1   Reliability analysis

To perform the reliability analysis, statistical information on the loads applied on the bridge and the resistance of the system are required. In this study, the resistance of the intact system is expressed in terms of the load multipliers LFu for the ultimate capacity, LF100 for the functionality criteria, and LF1 for member failure assuming linear elastic behavior. The load factors obtained from the nonlinear analysis express the capacity of the intact system to carry the live load. This capacity is a function of the applied dead load and the member resistance. Since these are random variables, then the capacity of the system is also random. For example, Equation 1 can be used to find the mean of LF1 and the COV given the means of R and D. DF1 and LLHS20 are taken to be deterministic variables. During the calibration of the AASHTO LRFD specifications, Nowak [8] found that the average member capacity of steel members is actually 1.12 times the nominal design capacity (resistance bias =1.12). The steel member resistances are also associated with a coefficient of variation COV equal to 10%. In addition, Nowak [8] assumes that the dead loads applied on the structure will have a bias that varies between 1.03 and 1.05 with a COV between 8% and 10%. Based on these observations it is herein assumed that on the average, the total combined dead load effects will have a bias on the order of 1.05 and a COV on the order of 10%.

Nowak [8] also assumes that the maximum lifetime (75 year) live loads (including dynamic impact) produce maximum moments which can be represented as multiples of the effects of the HS-20 trucks. Different factors are obtained depending on the span length. For example, for a 46 m (150 ft) bridge a factor equal to 2.01 is found. The 2.01 factor accounts for the dynamic impact as well as the static moment effect. Nowak [8] also assumes that the applied live load (including impact effect) is associated with a coefficient of variation equal to 19%. The 75 year lifetime load is used herein to find the reliability of the system against total collapse and against first member failure. Similar factors are provided for the two-year return period. These are used for the functionality criteria and the damaged condition.

The reliability calculations performed herein use the statistical information given above and assume that the LF1 factor follows a lognormal distribution while the applied load follows a Gumbel distribution. The calculation of the reliability of the whole system assumes that LFu follows a lognormal distribution and is associated with the same bias as that of LF1 and the same COV. This assumption is somewhat subjective but is based on the observation made by Cornell [10] about the relationship between the member resistances and the system's resistance. On the other hand, it is well known that the COV of the system is generally smaller than the COV of the individual members. However, this assumes that the structural model and system analysis process is exact. To account for the uncertainties in the structural modelling process while performing a nonlinear analysis, it is herein suggested to conservatively use a COV on LFu equal to the COV on the member resistances as represented by LF1. The same logic is followed while calculating the reliability index for the functionality and the damaged limit states.

The safety indices obtained for the 46 m (150 ft) bridges analyzed in this study for the intact ultimate capacity, β_u, and the functionality limit state, β_s, as well as the damaged bridge, β_d, conditions are given in reference [1]. These values are also compared to the member safety indices, β_{member}.

5.2 Determination of redundancy criteria

Reference [1] gives the reliability indices obtained in this study for the simple span steel bridges. The results show that for the ultimate limit state, the system reliability, β_u, is on the average higher than the member reliability, β_{member}, by 0.98 for all the 46 m simple span bridges considered. This means that $\Delta\beta_u$ (β_u-β_{member}), which is defined as a probabilistic measure of redundancy, is on the average equal to 0.98. Therefore, it is proposed to use a $\Delta\beta_u$, value of 1.0 (obtained by rounding up 0.98) as the redundancy criterion for the ultimate limit state. Thus, a bridge is defined as sufficiently redundant if the reliability index of the system is higher than that of the member by at least 1.0.

The average $\Delta\beta_s$ (β_s-β_{member}) value obtained for the 46 m simple span bridges studied for the functionality limit state is 0.91. Therefore, a $\Delta\beta_s$ value of 0.95 is used as the redundancy criterion for the functionality limit state. For the damaged limit state, the average difference $\Delta\beta_d$ (β_d-β_{member}) between the damaged system's safety index and the member safety index of the intact system is -2.04. Therefore, a value of -2.0 is used as the redundancy criterion for damaged bridges. The redundancy criteria chosen will be used in the next section as the target values during the calibration of the proposed system factors.

5.3 Calibration of system factors

System factors are calibrated such that bridges having configurations that do not provide sufficient levels of redundancy are penalized by requiring their individual members to provide higher levels of safety than those of bridges with sufficiently high levels of redundancy. On the other hand, bridges with high levels of redundancy are rewarded by allowing a lower level of member safety. This is performed by introducing system redundancy factors in the design or safety-check equations. The proposed format is such that:

$$\phi_s \, \phi R = \gamma_d \, D + \gamma_l \, L \tag{2}$$

where ϕ_s is the system redundancy factor, ϕ is the member resistance factor, R is the resistance capacity of the member, γ_d is the dead load factor, D is the dead load effect, γ_l is the live load factor, and L is the live load effect on an individual member (including dynamic impact). When ϕ_s is equal to 1.0, Equation (2) becomes the same as the current design equation. If ϕ_s is greater than 1.0 it indicates that the system's configuration provides sufficient level of redundancy. When it is less than 1.0 then the level of redundancy is not sufficient.

The redundancy criteria for $\Delta\beta_u$, $\Delta\beta_s$ and $\Delta\beta_d$ chosen in the previous section are used to calibrate system redundancy factors for each bridge configuration analyzed in this study. The procedure is performed such that bridges that produce $\Delta\beta_u$, $\Delta\beta_s$ and $\Delta\beta_d$ values less than the target values will be subjected to higher safety factors on their member resistances. The object is to increase their members' safety indices by the amounts $\Delta\beta_u$ - $\Delta\beta_{u\,target}$, $\Delta\beta_s$ - $\Delta\beta_{s\,target}$, and $\Delta\beta_s$ - $\Delta\beta_{s\,target}$. Different f_s values are calculated for each of the limit states studied.

Values of f_s factors for the 46 m simple span bridges with two-lanes of loading are shown in Table 3 for the three limit states studied. The results show that for a given beam spacing, the f_s factor (i.e. the bridge redundancy) increases as the number of beams is increased. This increase, however, reaches a plateau at 6 beams. Thus, no major improvement in bridge redundancy is observed when the number of members is increased beyond 6 beams.

		4 beams	6 beams	8 beams	10 beams
4ft	ultimate	0.84	1.03	1.05	1.05
	functi.	0.89	1.01	1.03	1.03
	damage	0.87	1.12	1.13	1.13
6 ft	ultimate	0.97	1.00	1.00	1.00
	functi.	0.97	1.00	1.00	1.00
	damage	0.84	0.95	0.96	0.95
8 ft	ultimate	0.99	1.00	1.00	1.00
	functi.	0.98	1.00	1.00	1.00
	damage	0.74	0.84	0.83	0.81
10 ft	ultimate	0.98	0.99	0.99	
	functi.	0.98	1.00	1.00	
	damage	0.58	0.63	0.62	
12 ft	ultimate	0.96	0.97		
	functi.	0.98	0.99		
	damage	0.46	0.52		

Table 3 *System factors for bridge redundancy*

The results also show that for a given number of beams, the ϕ_s factor increases as the beam spacing is increased from 1.2 m to 2.4 m (4 ft to 8 ft). However, the factor decreases as the beam spacing is increased beyond 2.4 m. This trend is explained by the fact that, for narrow bridges, all the beams are almost equally loaded and there is no reserve strength available. Hence, if one beam fails all the beams will quickly follow suit. However, as the beam spacing is increased, the load distribution is uneven and the least loaded members will pick up the load as the most heavily loaded member fails. As the spacing becomes very large, the capacity of the slab to transfer the load decreases and damage to the members under the applied load occur before a complete transfer to the other members is possible. This observation is evident because the nonlinear analysis performed herein considers the possibility of system damage before the formation of a plastic mechanism. Similar trends are observed for the ultimate limit state, the functionality limit state, or the damaged limit state. The trends are however the sharpest for the damaged limit state.

6. Conclusions

A method to account for bridge redundancy during the design and evaluation of bridge systems is proposed. The method consists of introducing system factors in the member design and evaluation equations. The factors are calibrated such that bridges that do not have sufficient levels of redundancy are penalized by requiring their members to have higher levels of safety than comparable redundant designs. On the other hand, bridges with high levels of redundancy are rewarded by allowing their members to have lower safety factors than normally required by current design and evaluation methods. Further work is underway to account for the results of the parametric analysis in the proposed framework.

Acknowledgements

References

1. GHOSN M. and MOSES F., "Redundancy in Highway Bridge Superstructures" Report NCHRP 12-36, TRB, Washington DC, March 1994.

2. HAMBLY, E.C., "Bridge Deck Behaviour", Chapman and Hall, Ltd., London, 1976.

3. ZOKAIE T., OSTERKAMP, T.A., and IMBSEN R.A., "Distribution of Wheel Loads on Highway Bridges", Final Report, NCHRP project 12-26/1, March 1991.

4. SCHILLING C.G., "A Unified Autostress Method", Project 51, Development of Design Specifications for Continuous Composite Plate-Girder Bridges, American Iron and Steel Institute, November 1989.

5. AASHTO, Standard Specifications for Highway Bridges, 15th. Ed., Wash. DC, 1992.

6. BURDETTE E.G. and GOODPASTURE, D.W., "Full Scale Bridge Testing - An Evaluation of Bridge Design Criteria", University of Tennessee, December 1971.

7. KATHOL S., AZIZINAMINI, A. and, LUEDKE, J., "Strength Capacity of Steel Girder Bridges", NDOR Research Project No. RES1 (0099) P469, Nebraska Department of Roads, February 1995.

8. NOWAK, A.S., "Calibration of LRFD Bridge Design Code", NCHRP 12-33, May 1992.

9. AASHTO, LRFD Bridge Design Specifications, First Edition, Washington DC, 1994.

10. CORNELL, C. A., "Risk-Based Structural Design", Proceedings of a Symposium on Risk Analysis, Department of Civil Engineering, University of Michigan, Ann Arbor, MI, August 1994.

Leere Seite

Blank page

Page vide

Stress Reduction due to Surfacing on Orthotropic Steel Decks

Henk KOLSTEIN
Research Engineer
Delft Univ. of Technology
Delft, The Netherlands

Henk Kolstein, born in 1952, joined Delft University of Technology in 1971. Since 1978 he has been participating in research within the domains of bridge loading and fatigue of orthotropic steel bridge decks
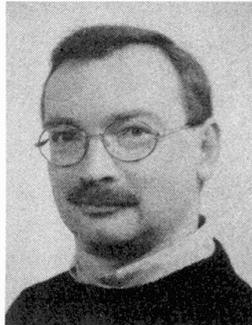
Jaap WARDENIER
Professor
Delft Univ. of Technology
Delft, The Netherlands

Jap Wardenier was born in 1943. As a consultant he has been involved in many projects. Since 1986, he is full time professor and Head of Steel and Timber Structures in the Faculty of Civil Engineering

Summary

The composite action between the steel deck plate of orthotropic bridge decks and the surfacing is an important aspect for the performance, since the stiffness of the combined unit reduces the strains in the welded structure as well as in the surfacing, resulting in a longer fatigue life. Since the stiffness behaviour of the bituminous surfacing is strongly influenced by temperature, loading frequencies and the composition of the total surfacing, the stress reducing effect in the steel components cannot easily be described and included in design rules. Excluding this effect for the calculated design life of the orthotropic decks gives considerable underestimation. On the other hand there is a tendency for the surfacing to crack above the longitudinal welds between the troughs and the deck plate. This paper reviews the numerical and experimental analysis of the composite action. It further highlights site measurements on two existing bridges for studying the temperature effect.

1. Introduction

1.1 Orthotropic steel bridge decks

Modern steel bridge decks consist of a 10-14 mm thick deck plate stiffened by 6 mm closed longitudinal stiffeners spanning in the direction of the traffic flow between the transverse stiffeners. Usually the deck plate of fixed bridges is surfaced with a 50-70 mm thick surfacing of e.g. mastic asphalt. As shown in Fig. 1 the so called orthotropic deck is a flexible structure which is highly sensitive to the local bending action produced by the wheel loads of heavy commercial vehicles. During its lifetime, the bridge steel deck including the surfacing can be expected to suffer many millions of cycles by wheel loading, so that fatigue is an important design criterion.
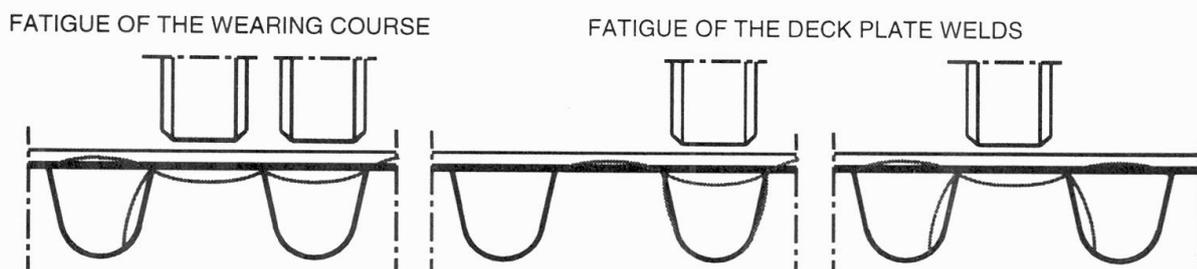
FATIGUE OF THE WEARING COURSE   FATIGUE OF THE DECK PLATE WELDS

Fig. 1 *Effects of local wheel loading on orthotropic steel bridge decks*

1.2 Desirable properties and qualities of the surfacing

The surfacing on the bridge requires an acceptable flexibility to ensure a good fatigue performance and it is equally important that the surfacing possesses enough resistance against rutting of the wheel loads. Extensive deformations of the surfacing results in high and unacceptable dynamic effects in the steel deck. Further the steel deck has to be protected against corrosion by one of the layers in the surfacing. Nowadays porous wearing courses are very popular in The Netherlands [5, 7]. The reason for this is mainly, that they give comfort to the use of the road. They have a high skid resistance, they reduce the noise nuisance, prevent splash and spray water, while aquaplaning is in principle impossible.

1.3 Composite action between steel deck and surfacing

The composite action between the steel deck plate of orthotropic bridge decks and the surfacing is an important aspect of the performance, in particular because the stiffness of the combined unit reduces the strains in the welded structure as well as in the surfacing, which results in a longer fatgue life.
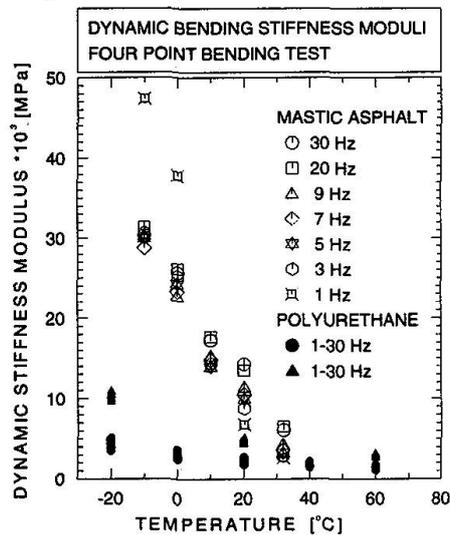
Fig. 2 Bending stiffness moduli

1.3.1 Dynamic bending stiffness moduli

Since the stiffness behaviour (Fig. 2) of the bituminous wearing course is strongly influenced by temperature, loading frequencies and composition of the total surfacing, the stress reducing effect in the steel components cannot easily be described and included in design rules.

Recently developed surfacing systems using polyurethane binders show dynamic stiffness moduli of a rather constant value, especially at temperatures above zero degrees. At low temperatures the values are considerably lower than the systems using bitumen binders.

1.3.2 Fatigue assessment of welded connections

A summary of fatigue lifes of several connections in orthotropic steel bridge decks for particular loads have been published by Gurney [4] and are partly shown in Table 1. All lives relate to a 2.3% probability of failure and a traffic flow of 800.000 lorries per annum. It can be seen that, for the unsurfaced deck, none of the details met the 120 years design life required by the Britsh Standard.

Joint (weld class-BS5400)	Unsurfaced deck	Surfaced deck
Stiffener to deck (F)	6.5	94
Longitudinal butt weld (F)	5.9	>120
Web of box to deck (D)	41	>120
Stiffener to crossbeam (G)	4.3	13
Crossbeam to deck (D)	94	>120
Transverse butt weld (F)	35	>120

Table 1 Fatigue life of joints (years) by Gurney [4]

1.3.3 Durability of the surfacing

There is a tendency for the surfacing to crack above the longitudinal welds between the troughs and the deck plate. To maximise the period between the costly and traffic-disruptive resurfacing operations less traffic susceptible systems have to be applied. Full scale tests carried out by Kolstein and all. [6] on several types of surfacing systems showed that an improved wearing course can only result in a longer life if the dynamic bending stiffness modulus is at least equal to that of the conventional systems and the fatigue strength of the wearing course is higher than the conventinal one.

2.   Theoretical analysis of the composite action

The composite effect has been calculated by Kolstein [7] for different steel plate thicknesses (10-16 mm) and layer thicknesses (5-80 mm), various dynamic stiffness moduli (1.000-30.000 MPa) and the effect of the interlayer (flexible or stiff). The model used consists of a beam which is loaded by a constant moment which results in 70 MPa for a 12 mm steel plate without surfacing. The strains for a flexible and a stiff interface between the steel and the wearing course are shown in Fig. 3. for locations at the underside of a 12mm steel plate and the topside of the wearing course. The results for different thicknesses of the steel plate in combination with a 50mm surfacing are given in Fig. 4.
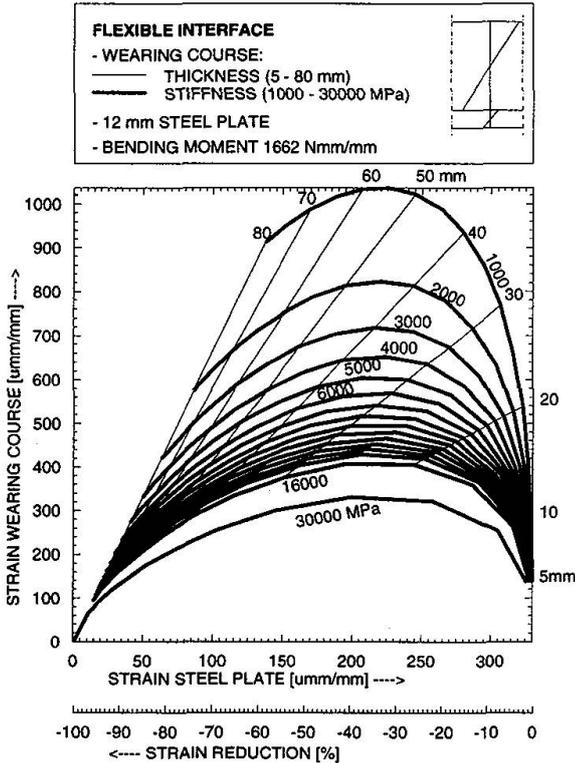
Fig. 3a *Strains assuming a flexible interface.*
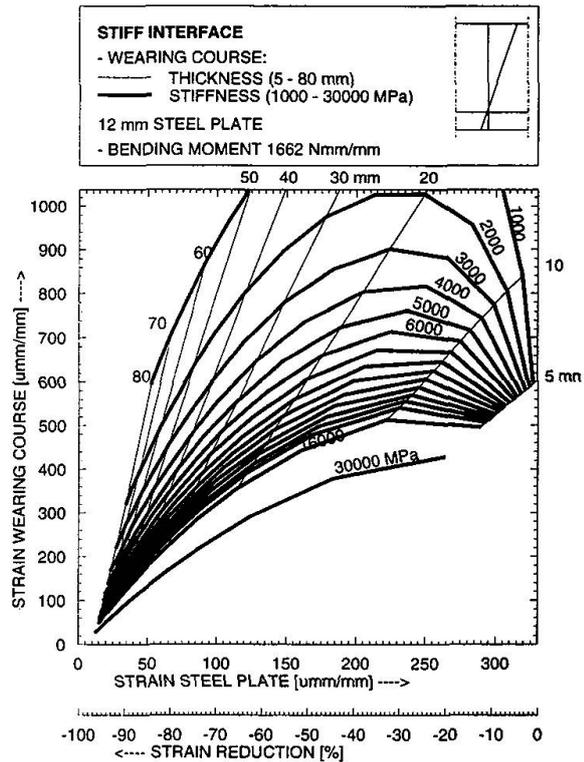
Fig. 3b *Strains assuming a stiff interface.*
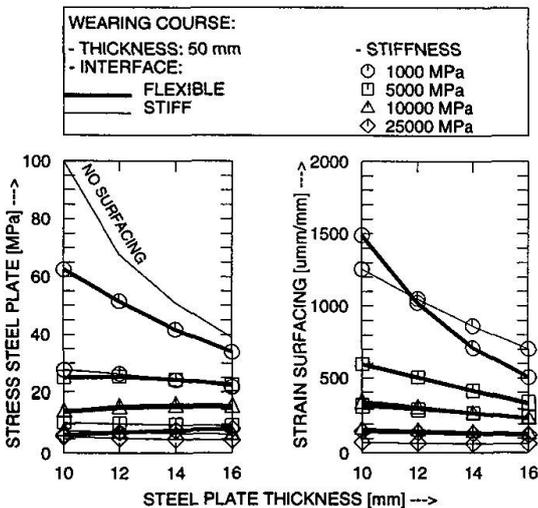
Fig. 4 *Influence of steel plate thickness*

As shown in Fig. 2 the dynamic stiffness moduli of the wearing couse at low temperatures is relative high (25000-30000 MPa) and at higher temperatures relative low (2000-5000 Mpa). From Fig 3 it can be seen e.g. that for a 50mm surfacing the strain reduction in the steel as well as in the surfacing at low temperatures is very high (±90%). At higer temperatures the strain reduction in the steel plate is still exceeds 40% and in the surfacing limited to about 20%. From Fig. 4 it can be concluded that the influence of the steel plate thickness is relatively small. The thickness and the stiffness of the wearing course as shown in Fig. 2 and 3 are much more important. Tests carried out by Kolstein [6] showed that for mastic asphalt systems the interlayer between the wearing course and the steel behaves stiff at temperatures below 20°C and relatively flexible above 20°C.

3. Laboratory tests with respect to the composite action

The effects of the surfacing on the stresses in the steel deck have been investigated by Smith et all. on a full scale section of a steel deck of Vee-stiffeners [9]. Static as well as dynamic loading arrangements in the surfaced and unsurfaced condition were carried out (see Fig. 5). Under dynamic loading, which refers to a pulse duration of 0.1sec, stress reduction of about 64-84% at 35°C have been found in a 12mm steel deck due to the composite effect of the 50mm asphalt surfacing (see Table 2). At 15°C and -5°C the stress reduction were about 84-98%.
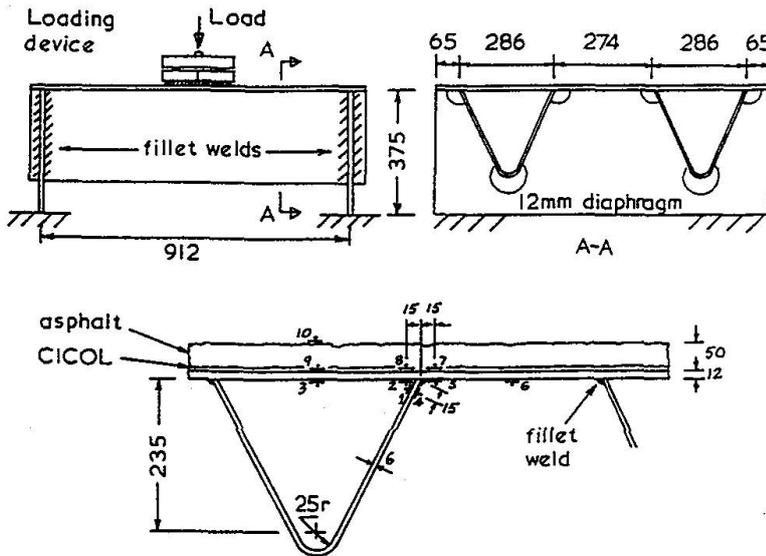
Fig. 5 Full scale test by Smith et all. [9]

Gauge	35°C	15°C	-5°C
1	0.23	0.16	0.11
2	0.23	0.12	-0.16
3	0.30	0.15	0.12
4	0.20	-0.12	-0.14
5	0.36	0.09	0.02
6	0.16	0.05	~0.0
7	0.29	0.02	~0.0
8	0.36	0.11	0.06

Table 2 Reduction factors [9]

Comparible stress reductions were found by Kolstein [6] testing specimens in a temperature range of -25°C up to +40°C. The load signal used has been obtained by analysing strain gauge measurements on an existing bridge.

In this research program also tests have been carried out to improve the fatigue resistance of the traditional mastic asphalt by using modified bitumen. Fatigue test results on two types of mastic asphalt are shown in Fig. 6a and 6b. The dynamic stiffness modulus of the modified type (STY-P1) appeared to be lower than the traditional one (REFB-P1). Considering the results in terms of applied strains the fatigue strength of the modified type is better. However if the results are plotted in terms of applied stresses just the opposite was found. In Fig. 6c the effect of these two materials on a steel deck are shown. It can be noticed that the modified type (STY1) resulted in larger deformations of the steel plate and a fatigue behaviour comparable to the traditional one (REF2). So it was concluded that due to the composite effect it is necessary to require for a modified surfacing layer, besides a better fatigue resistance, at least stiffness moduli which is the same as that of a traditional used surfacing system.
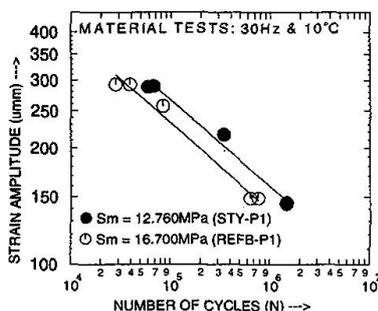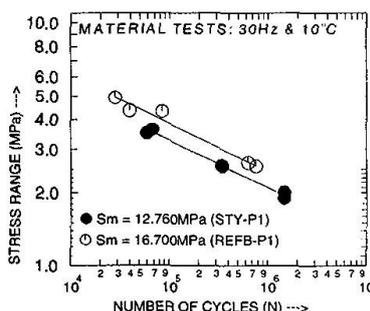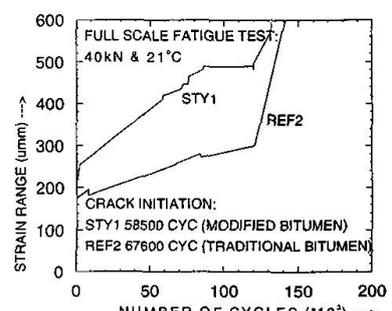

Fig. 6a

Fig. 6b

Fig. 6c

4.   Site measurements

To obtain information about the composite action of the surfacing on real structures site measurements have been carried out on two highway bridges in The Netherlands. On the first bridge strain measurements have been performed on the unsurfaced bridge deck and the surfaced bridge deck with different surfacing systems (mastic asphalt and a polyurethane system) using a calibrated truck as well as under normal traffic conditions. On the second more heavily loaded bridge strain measurements took place at more locations of the orthotropic deck which have been built up with various plate thicknesses. First results have been published by Kolstein et all. earlier [6, 9]. In this paper the authors concentrate on the influence of the temperature and the steel plate thickness on the stress spectra measured under normal traffic conditions.

4.1   Description and instrumentation of the bridges

4.1.1   Steel structure, surfacing and traffic intensity

The Caland Bridge (Fig. 7) built in 1969 is an important link in the habour area of Rotterdam. It has four traffic lanes, two railway tracks, a bicycle track and a foot path. It is a plate girder truss bridge with four spans. One of them is a vertical lift bridge. The road section consists of a 10mm steel deck plate with closed longitudinal stiffeners. The original surfacing system was based on bitumen binders (mastic asphalt). A part of the surfacing has been replaced by a new system based on polyurethane resins. In both cases the nominal thickness of the total surfacing amounts to 50mm.

The Moerdijk Bridge (Fig. 8) built in 1975 carries the long distance traffic to e.g. Belgium, France and Spain. The truck intensity in the order of 2.10^6 per year in each direction is divided over three traffic lanes. This box girder bridge has 10 independend spans of 100m. The bridge deck consists of an orthotropic steel plate of 10, 12 and 14mm (varying in longitudinal direction) stiffened by trapezoïdal longitudinal stiffeners. The nominal thickness of the mastic asphalt surfacing system is 60mm.
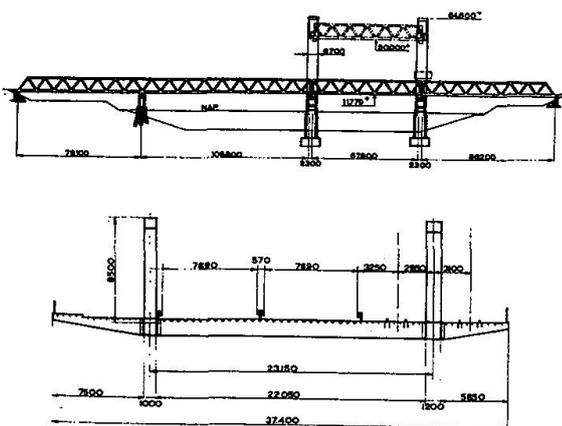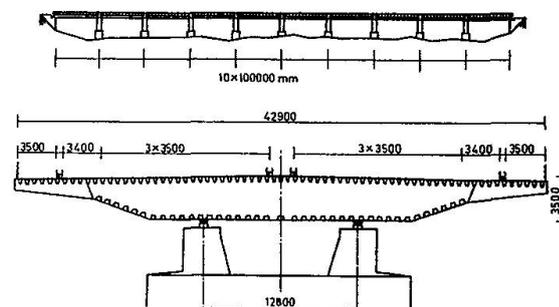

Fig. 7 Calandbridge

Fig. 8 Moerdijk Bridge

4.1.2   Instrumentation and processing of the data

In several sections of the bridges, various strain gauges were applied in order to obtain an insight in the effect of the surfacing in reducing the strains in the steel deck plate. Most strain gauges were positioned 25mm from the welds between the deck plate and the longitudinal stiffeners, and close to the offside wheel track of the heavy loaded slow lane. Several temperature gauges were

attached to the underside of the steel deck plate. Only the locations further discussed in this paper are indicated in Fig. 9.

(a) Caland Bridge   (b) Moerdijk Bridge

Fig. 9 Strain gauge locations
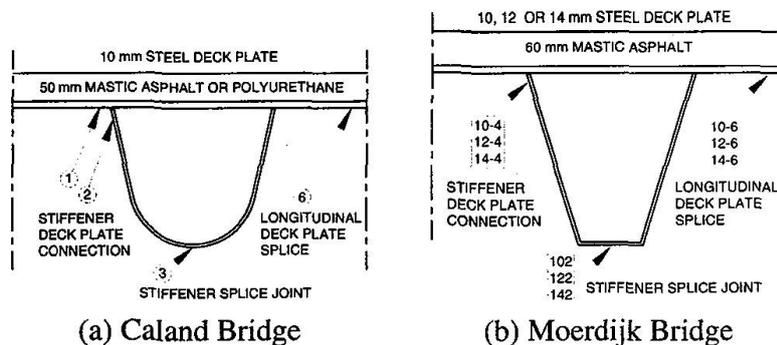
The stress variations have been measured under normal trafficking. The range-pair cycle counting method has been used to convert the stress spectra of a complex waveform into a sequence of identifiable cycles to enable Miner's rule to be used to calculate the fatigue damage produced by the spectrum.

4.1.3 Test results

Stress spectra measured on the Moerdijk Bridge at several locations and different cross sections (deck plate of 10, 12 and 14mm) have been summarised in Fig. 10, 11 and 12. These measurements have been carried while the temperature at the underside of the deckplate amounts to be about 35°C (July 95), about 15°C (Nov 94) and respectively 5°C (Febr 94). As mentioned before the thickness of the mastic asphalt surfacing is about 60mm.

For the stiffener deck plate connection (Fig. 10) and the longitudinal deck plate splice (Fig.11) it can be seen that at these locations the influence of the temperature on the stress level is larger than the influence of the thickness of the steel deck. A thicker deck plate reduces the stresses effectively if the temperature is high. This agrees with the conclusions of the theoretical analysis as shown before in Fig. 4. The stress spectra measured at the bottomside of the longitudinal stiffener splice joint (Fig. 12) are less influenced by the temperature. Here there is some influence of the thickness of the steel deck plate.

Using the stress spectra measured in July 95 for the different welded connections the fatigue damage as a function of the fatigue categories according to the ECCS recommendations or Eurocode design rules have been calculated. The results are gathered in Fig. 13 and Fig. 14. From Fig. 13 the effect of the steel plate thickness can be seen clearly. For the stiffener splice joint the effect is neglectible. For the stiffener to deck joint and the longitudinal butt weld the effect is clearly visible. From Table 3 it can be seen that a 20% thicker deck plate reduces the fatigue damage with a factor 1,7 to 5,1. For a 40% thicker plate this factor is about 3,4 to 8,0.

Joint (fatigue class)	Deck plate thickness		
	10mm	12mm	14mm
Stiffener to deck joint			
(EC3-100)	$11,3.10^{-5}$	$4,13.10^{-5}$	$1,42.10^{5}$
(EC3-56)	$15,2.10^{-4}$	$7,60.10^{-4}$	$4,50.10^{4}$
Longitudinal deck plate splice			
(EC3-100)		$3,60.10^{-4}$	$1,36.10^{4}$
(EC3-71)		$4,00.10^{-3}$	$7,79.10^{4}$

Table 3 Fatigue damage (D3+D5), spectra Moerdijk Bridge over the month July 95
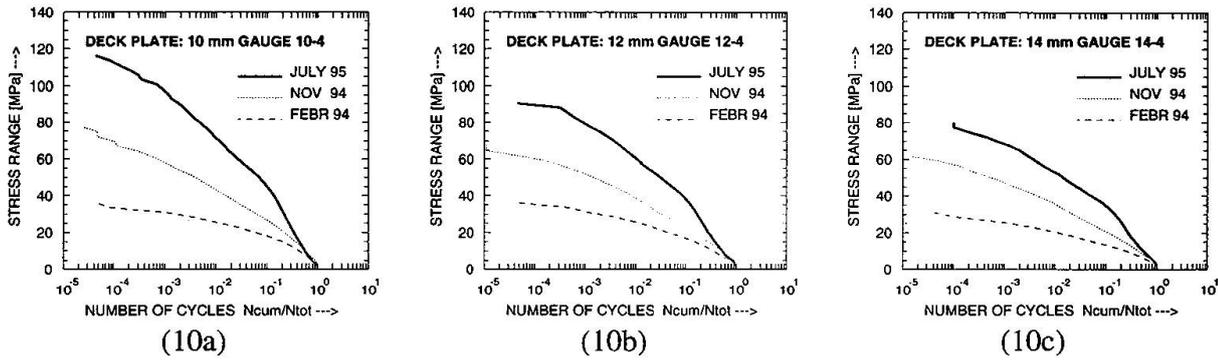
Fig. 10 Measured stress spectra _stiffener deck plate connection_ - 60mm mastic asphalt surfacing
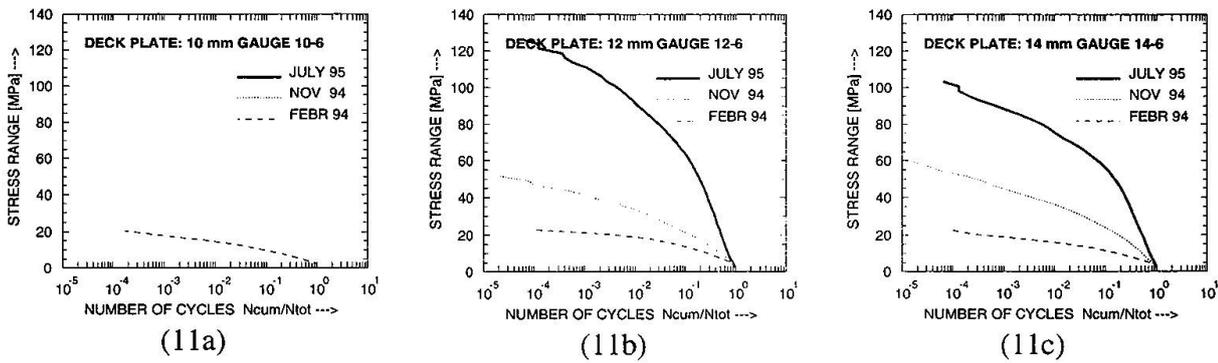

Fig. 11 Measured stress spectra _longitudinal deck plate splice_ - 60 mm mastic asphalt surfacing
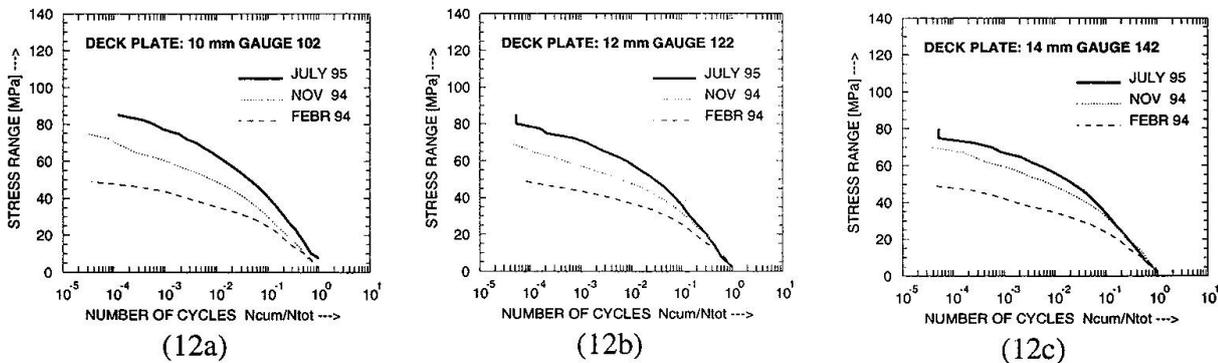

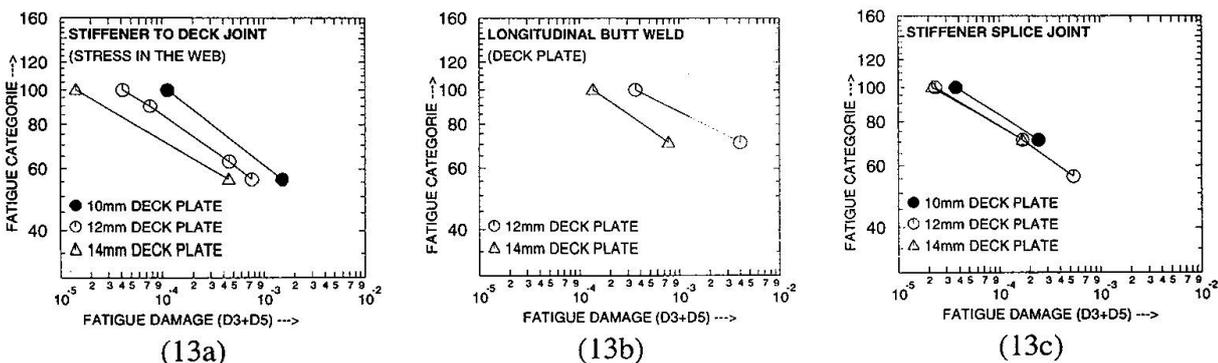Fig. 12 Measured stress spectra _stiffener splice joint_ - 60mm mastic asphalt surfacing

Fig. 13 Damage calculations using EC3 fatigue categories and stress spectra of July 95 .
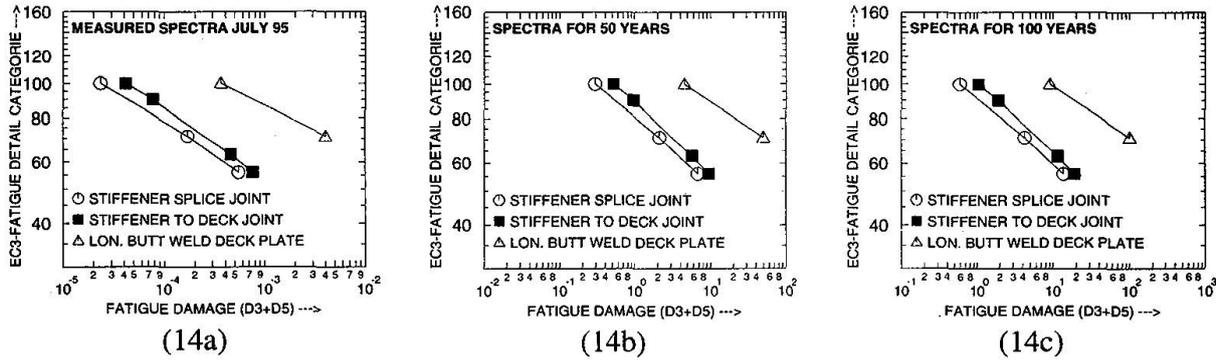
(14a)   (14b)   (14c)

Fig. 14 Damage calculations using EC 3 fatigue categories and stress spectra based of July 95

Considering the fatigue damage for the three different details for the 12 mm deck plate only, from Fig. 14 it can be concluded that the fatigue damage for the longitudinal butt weld in the deck plate is much higher than the fatigue damage for the other two details.

Joint	EC3-Fatigue Detail Category	
	50 years	100 years
Stiffenener splice joint	80	90
Stiffener to deck joint	90	100
Longitudinal deck platesplice	125	140

Table 4. Required EC3-fatigue detail category

If the measured spectra in July would be representive for the whole life time of the bridge the calculated fatigue damage can be related to a number of years (see Fig. 14b and Fig. 14c). For a "crack free period" of 50 years or 100 years the required fatigue detail categories for the different joints can be calculated and are given in Table 4.

If the results of the stresses measured in e.g. FEBR 94 and NOV 94 (see Fig. 10, 12 and 13) are included in the year spectrum it is clear that the required fatigue categories from Table 4 are much too conservative. The resulting spectra are at such a level that depending on the considered fatigue class all stress ranges are below the constant amplitude fatigue limit. Here the fatigue damage very small or even neglectable.

4.1.3.2 Comparison of stress spectra using different surfacing systems (50mm thickness)

Stress spectra measured on the Caland Bridge at several loctions are given in Fig. 15. It can be seen that at a temperature domain of -5°C up to +23,4°C the stress spectra are influenced only slightly by the level of temperature under the surfacing system which is based on synthetic materials. It is clear that if the stress reducing effect is included in design rules the behaviour of different systems must be included in a proper way.
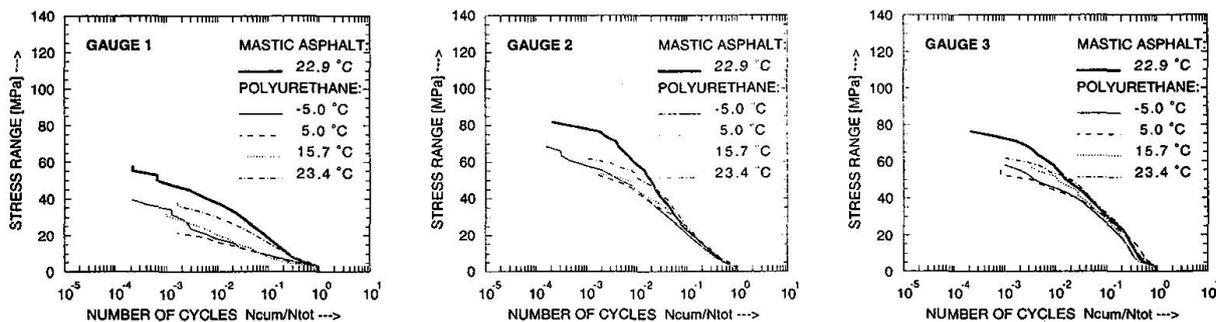

Fig. 15 Measured stress spectra Caland bridge 10 mm deck plate and 50 mm surfacing

5. European Prestandards

5.1 ENV 1991-3 Traffic Loads on Bridges

The dispersal through the pavement and orthotropic decks of the concentrated loads (wheel contact area) of the load models mentioned in Eurocode 1 Part 3 is taken at a spread-to-depth ratio of 1 horizontally to 1 vertically down to the level of the middle plane of the structural top plate below. This rule is only valid for the characteristic loads intended for the determination of road vehicle effects associated with ultimate limit-state verifications and with particular serviceability verifications. This is not applicable for the fatigue load models.

5.2 Draft ENV 1993-2 Steel Bridges

In the current draft of Eurocode 3 Part 2 the longitudinal stiffeners or stringers have to be designed for a minimum stiffness to reduce the flexibility of the steel deck especially close to a hard line support such as a web of a main girder. The required stiffness will be higher for stiffeners adjacent to a web, to reduce the relative deflections and hence the flexural strains in the surfacing. However in the code up to now rules are missing which take count of the composite action of the surfacing with the deck plate.

6. Concluding Remarks

It can be concluded that measurements on existing bridges confirm the theoretical analysis and laboratory tests carried with respect to the composite effect of the surfacing and the orthotropic steel bridge deck. This means that the influence of the thickness of the steel plate is low compared to the influence of the temperature on the composite action of the surfacing and steel plate. Furthermore the behaviour of bituminous surfacing systems differ from systems based on synthetic materials. To be able to quantify the composite action additional measurements and further parametric studies are required. For the design of new bridges and the evaluation of existing bridges it is required to include this effect in the fatigue analysis of welded details of orthotropic steel decks.

Neglecting the surfacing provides a factor of safety of unknown magnitude. If the contribution of the surfacing could be quantified it is possible to take it into account for design purposes, thus leading to a more efficient and hence cheaper structure, although adequate maintenance (including replacement) would be necessary to ensure that its contribution remains effective through the life of the bridge.

Recently in the Netherlands an orthotropic steel deck plate with a thickness of 18 mm and an 8 mm thick synthetic resin wear layer has been built. Compared to an asphalt mastic layer, this provides considerable savings on the structures own weight.

7. Acknowledgements

References

1. BROWN, C.W., ILES, D.C. Design of Steel Bridges for Durability, SCI publication 154, The Steel Construction Institute, Ascot, ISBN 185942 0281, 1995.

2. CULLIMORE, M.S.G., FLETT, I.D., SMITH, J.W. Flexture of Steel Bridge Deck Plate with Asphalt Surfacing. IABSE Periodica 1/1983. 1-15, 1983.

3. GUNTHER, G.H., BILD, S., SEDLACEK, G. Durability of Asphalt Pavements on Orthotropic Decks of Steel Bridges. J. Construct. Steel Research, 7, 85-106, 1987.

4. GURNEY, T. Fatigue of Steel Bridge Decks. TRL State of the Art Review 8. HMSO Publications Centre, London, ISBN 0 11 551141 5, 1992.

5. HOPMAN, P.C., COORENGEL, R. Development of a Drain Asphalt Concrete Wearing Course for an Orthotropic Steel Bridge. In: Proceedings 4th Eurobitume Symposium. Madrid, 921-924, 1989.

6. KOLSTEIN, M.H., DIJKINK, J.H. Behaviour of Modified Bituminous Surfacings on Orthotropic Steel Bridge Decks. In: Proceedings 4th Eurobitume Symposium. Madrid, 908-915, 1989.

7. KOLSTEIN, M.H. New Development of a Porous Wearing Course for Steel Orthtropic Bridge Decks based on Synthetic Materials. In: Building the Future, Innovation in design, materials and construction. Chapman & Hall, 141-149, 1994.

8. KOLSTEIN, M.H., WARDENIER, J. Composite Action of the Surfacing on Steel Orthotropic Bridge Decks. In: Proc. 4th Pacific Structural Steel Conference, Singapore, Pergamon, 613-621,1995.

9. SMITH, J.W., CULLIMORE, M.S.G. (1987). Stress Reduction due to Surfacing on a Steel bridge Deck. In: Int. Conf. Steel and Aluminimum Structures. Elsevier, 806-816, 1987.

10. SMITH, J.W. Asphalt Paving for Steel Bridge Decks. In: Proceedings Annual Meeting of the Association of Asphalt Paving Technologits. Reno, Nevada,1987.

11. ENV 1991-3, Eurocode 1: Basis of Design and Actions on Structures Part 3: Traffic Loads on Bridges, European Committee for Standardisation, Brussles, 1995.

12. DRAFT ENV 1993-2, Eurocode 3: Design of Steel Structures Part 2: Steel Bridges, European Committee for Standardisation, Brussels, 1996.